



## TUMORIGENESIS AND NEOPLASTIC PROGRESSION

# Sustained Inhibition of NF- $\kappa$ B Activity Mitigates Retinal Vasculopathy in Diabetes



Rubens P. Homme,<sup>\*†</sup> Harpal S. Sandhu,<sup>‡§</sup> Akash K. George,<sup>\*†</sup> Suresh C. Tyagi,<sup>†</sup> and Mahavir Singh<sup>\*†</sup>

From the Eye and Vision Science Laboratory,<sup>\*</sup> the Departments of Physiology<sup>†</sup> and Ophthalmology and Visual Sciences,<sup>‡</sup> and the Kentucky Lions Eye Center,<sup>§</sup> University of Louisville School of Medicine, Louisville, Kentucky

Accepted for publication  
January 20, 2021.

Address correspondence to  
Mahavir Singh, D.V.M., Ph.D.,  
Eye and Vision Science Laboratory,  
Department of Physiology,  
University of Louisville School of  
Medicine, Health Sciences Center,  
Room 1216, 500 S. Preston St.,  
Louisville, KY 40202. E-mail:  
[mahavir.singh@louisville.edu](mailto:mahavir.singh@louisville.edu) or  
[gene2genetics@gmail.com](mailto:gene2genetics@gmail.com).

This study investigated the effects of long-term NF- $\kappa$ B inhibition in mitigating retinal vasculopathy in a type 1 diabetic mouse model (Akita, Ins2<sup>Akita</sup>). Akita and wild-type (C57BL/6J) male mice, 24 to 26 weeks old, were treated with or without a selective inhibitor of NF- $\kappa$ B, 4-methyl-N1-(3-phenyl-propyl) benzene-1,2-diamine (JSH-23), for 4 weeks. Treatment was given when the mice were at least 24 weeks old. Metabolic parameters, key inflammatory mediators, blood-retinal barrier junction molecules, retinal structure, and function were measured. JSH-23 significantly lowered basal glucose levels and intraocular pressure in Akita. It also mitigated vascular remodeling and microaneurysms significantly. Optical coherence tomography of untreated Akita showed thinning of retinal layers; however, treatment with JSH-23 could prevent it. Electroretinogram demonstrated that A- and B-waves in Akita were significantly smaller than in wild type mice, indicating that JSH-23 intervention prevented loss of retinal function. Protein levels and gene expression of key inflammatory mediators, such as NOD-like receptor family pyrin domain-containing 3, intercellular adhesion molecule-1, inducible nitric oxide synthase, and cyclooxygenase-2, were decreased after JSH-23 treatment. At the same time, connexin-43 and occludin were maintained. Vision-guided behavior also improved significantly. The results show that reducing inflammation could protect the diabetic retina and its vasculature. Findings appear to have broader implications in treating not only ocular conditions but also other vasculopathies. (*Am J Pathol* 2021, 191: 947–964; <https://doi.org/10.1016/j.ajpath.2021.01.016>)

Type 1 diabetes (T1D) is a chronic illness typically diagnosed during childhood. It occurs in approximately 1:400 to 600 US children.<sup>1</sup> A recent trend shows a disturbing 15% to 20% increase in new diagnoses of T1D for those aged <5 years.<sup>2,3</sup> The reason for this alarming increase is debatable. Clinically, the management of T1D has proved to be challenging for a variety of reasons, including physiological factors such as increased insulin sensitivity, especially in children.<sup>4</sup> T1D is an inflammatory disease with microvascular complications that leads to diabetic retinopathy (DR).<sup>5</sup> DR is generally divided into nonproliferative diabetic retinopathy, an early stage wherein symptoms can be mild, moderate, or nonexistent. It is marked by the presence of microaneurysms, which may leak fluid into the retina.<sup>6</sup> Furthermore, the blood-retinal barrier (BRB) breakdown exacerbates capillary permeability, contributing to swelling of the macula lutea, also called fovea (a part of the retina, responsible for sharp and detailed central vision;

the visual acuity). Without intervention, the disease can transition to proliferative diabetic, a progressive condition wherein the ischemic retina stimulates angiogenesis to drive neovascularization. If left untreated, proliferative diabetic retinopathy can cause severe vision loss or permanent blindness.

DR has become a leading cause of blindness in working-age adults globally.<sup>7,8</sup> Current interventions do not adequately address the retinovascular signature pathology that underlies initiation, progression, and maintenance of DR phenotype. Furthermore, they fail to restore vision loss in many patients. DR's etiology remains enigmatic despite

Supported by NIH grants HL139047, AR071789, HL74815, HL107640, HL139047, and DK116591 (S.C.T.).

Disclosures: None declared.

Portions of this work were presented at Experimental Biology 2018: April 21 to 25, 2018, in San Diego, CA; and Experimental Biology 2019: April 6 to 9, 2019, in Orlando, FL.

an abundance of literature describing the impact of polyol, hexosamine pathway, advanced glycation end products, and oxidative stress. Of late DR is being considered as an inflammatory disease because a variety of inflammatory mediators have been detected in diabetic animal and human vitreous and their retinæ.<sup>9</sup> Interestingly, a substantial increase in inflammatory mediator expression is also directly associated with NF- $\kappa$ B (nuclear factor  $\kappa$ -light-chain enhancer of activated B cells).<sup>10</sup> Briefly, the nuclear factor- $\kappa$ B is a dynamic transcription factor that orchestrates complex biological processes, including the immune system inflammatory response.<sup>11</sup> Because of its upstream role in cell signaling, NF- $\kappa$ B remains a central component in inflammation. It induces cytokines and responds to stress, free radicals, heavy metals, UV irradiation, oxidized low-density lipoprotein, and bacterial and viral antigens.

NF- $\kappa$ B is a first responder to harmful stimuli; it shuttles between cytoplasm and nucleus to initiate and then help execute a robust gene-transcription program. It consists of a family of transcription factors: NF- $\kappa$ B1 (p50), NF- $\kappa$ B2 (p52), RelA (p65), RelB, and c-Rel. These alone or together form heterodimers and homodimers that translocate to the nucleus. They then bind to specific DNA sequences to promote the expression of inflammatory mediators.<sup>12–15</sup> The most prevalent heterodimer of the NF- $\kappa$ B family, p65/p50, plays a significant role in the inflammatory response. Recently, 4-methyl-N1-(3-phenyl-propyl) benzene-1,2-diamine (known as JSH-23) was used to inhibit the nuclear translocation of the p65/p50 heterodimer.<sup>16</sup> JSH-23 inhibits translocation of NF- $\kappa$ B in RAW 264.7 cells stimulated by lipopolysaccharides.<sup>14,17</sup> JSH-23 is cell permeable and is also effective in mitigating microvascular complications (eg, neuropathy).<sup>13,14</sup>

This study aimed to determine the role of inflammation in remodeling of retinal structure and function in the Akita mouse strain and investigate whether JSH-23 can protect the diabetic retina. Hyperglycemia in T1D induces retinal inflammation via NF- $\kappa$ B activation. Retinal capillary endothelial cells, pericytes, and glial cells are critical parts of the BRB. They are potential targets of inflammatory mediators. These mediators also target junctional molecules, thus impairing cell-cell communication and paracellular transport. NF- $\kappa$ B activation increases the expression of proinflammatory genes that induce BRB breakdown.<sup>18–22</sup> Therefore, preempting inflammation on a long-term basis by inhibiting NF- $\kappa$ B activity may mitigate microvascular alterations in the diabetic retina. The Ins2Akita mouse strain (Akita) was used to test this hypothesis. It is characterized as a T1D model because of its fertility, stable insulin-deficient diabetes, and no systemic immune modulation.<sup>23</sup> Akita harbors a missense mutation in the insulin 2 gene, leading to a conformational change in the insulin protein, causing its accumulation in the pancreatic  $\beta$  cells. Accumulation of misfolded insulin causes severe hyperglycemia-induced inflammation due to loss function, decreased density, and death of  $\beta$  cells.<sup>23–26</sup> This hyperglycemia-induced

pathology ensues with a parallel increase in acellular retinal capillaries, infiltration of leukocytes into vascular walls, thinning of the inner retinal layers, and apoptosis of retinal cells.<sup>23,27,28</sup>

## Materials and Methods

### Animal Genotyping and Maintenance

Akita (T1D Ins2<sup>Akita/+</sup>) mice were characterized by chronic hypoinsulinemia and hyperglycemia. They usually develop spontaneous diabetes by 4 weeks of age. They were purchased from the Jackson Laboratory (Bar Harbor, ME). Male Akita mice, 24 to 26 weeks old, were used throughout the experiments. To maintain a consistent background, wild-type (WT) littermate male mice that lack the Ins2<sup>Akita</sup> mutation were used as control. All animals were kept in a 12:12-hour light-dark cycle with a regular mouse diet at the University of Louisville School of Medicine animal facility. According to Association for Research in Vision and Ophthalmology guidelines, mice were cared for, as approved by the Institutional Animal Care and Use Committee of the University of Louisville, Louisville, KY. The experimental protocols were performed following the NIH *Guide for the Care and Use of Laboratory Animals*.<sup>29,30</sup> Genotyping of the mice was performed by collecting the tail biopsy, as previously reported.<sup>31</sup> DNA was isolated using DNeasy blood and tissue kit (Qiagen, Germantown, MD). The cross-breeding yields Ins2<sup>Akita</sup> with high and low glucose levels, measured by blood glucose meter Ultra Touch 2 (Life Scan, Malvern, PA). High glucose level was defined as >300 mg/dL. Low glucose level was defined as  $\leq$ 250 mg/dL. Only mice with high glucose levels were used in the study.

### Study Protocol

Mice were divided into four different groups: i) WT, ii) WT + NF- $\kappa$ B inhibitor (JSH-23), iii) Ins2<sup>Akita</sup>, and iv) Ins2<sup>Akita</sup> + JSH-23. The NF- $\kappa$ B inhibitor (JSH-23) was purchased from Sigma Aldrich (St. Louis, MO; Chemical Abstracts Service number 749886-87-1). Depending on the experiment's nature, a minimum of 5 to 20 mice was used in each group. A stock solution of JSH-23 was prepared by diluting 25 mg JSH-23 in 1000  $\mu$ L of 200 proof ethanol (Decon Labs, King of Prussia, PA; CAS number 64-17-5), and stored at  $-70^{\circ}\text{C}$ . A total of 100  $\mu$ L of the stock solution was then diluted with 4900  $\mu$ L of 1 $\times$  sterile phosphate-buffered saline. The control solution was prepared with 4900  $\mu$ L of 1 $\times$  phosphate-buffered saline and 100  $\mu$ L of 200 proof ethanol. Akita and WT mice strains were treated with or without the specific inhibitor, JSH-23, intraperitoneally at 5 mg/kg body weight on alternate days for a total of 4 weeks. The treatment started once the mice were approximately 26 weeks old. The treatment protocol was chosen because of the following reasons: i) higher

concentrations, such as 10 or 20 mg/kg body weight, were toxic, ii) JSH-23 dissolved in dimethyl sulfoxide was toxic, iii) no study has reported the toxicity of JSH-23 at a higher concentration or its dilution in dimethyl sulfoxide, although a study that used higher concentration was performed for a week,<sup>32</sup> and iv) previous studies primarily chose alternate days, and 2 weeks was the most common duration.

### Measurement of Blood Glucose, Glucose Tolerance Test, Blood Insulin, Body Weights, Systemic Blood Pressure, and Recording of Intraocular Pressure

Blood glucose was measured with Ultra Touch 2 Glucometer (LifeScan, Malvern, PA) before and after treatment with or without JSH-23. A glucose tolerance test was performed to measure the clearance of intraperitoneally injected glucose load from the body and to detect disturbances in glucose metabolism linked to diabetes. Both WT and Akita mice fasted for 5 hours before basal blood glucose levels were determined. Glucose was then administered by i.p. injection. Subsequently, the blood glucose levels were measured at 30-minute intervals for 2 hours.<sup>33,34</sup> The plasma insulin levels were also measured to understand glucose metabolism. Mouse INSULIN ELISA kit (EMINS) from Thermo Fischer Scientific (Waltham, MA) was used to analyze plasma insulin levels. The test was performed according to the manufacturer's instructions.<sup>35</sup> Body weights of all the animals were recorded using an electronic weighing balance, OHAUS, CS-2000 (Sigma Millipore, St. Louis, MO). Systemic blood pressure was measured with CODA noninvasive blood pressure instrument (CODA Instrument, Ken Scientific, Torrington, CT).<sup>36</sup> The intraocular pressure (IOP) was recorded by a tonometer before and after JSH-23 treatment (iCare, Tonolab, Raleigh, NC).<sup>37</sup>

### In Vivo Fluorescence Angiography

Mice were injected intraperitoneally with 100 µL of AK-FLUOR (NDC 17478-253-10; Akorn, Inc., Lake Forest, IL) after induction of anesthesia with 300 µL of 2× tribromoethanol. The fundus was visualized by a

Micron IV microscope (Phoenix Technology Group, Pleasanton, CA). Images were analyzed via ImageJ software version 1.x (NIH, Bethesda, MD; [https://imagej.net/imagej\\_1.x](https://imagej.net/imagej_1.x), last accessed April 14, 2018)<sup>30</sup> for the presence of fluorescence outside of the retinal capillaries.<sup>37</sup> The capillary (the space between the retinal veins and retinal arteries) area in the fluorescence angiography (FA) picture was highlighted and quantified as fluorescence intensity (arbitrary units).<sup>38,39</sup>

### In Vivo ERG and OCT

Electroretinograms (ERGs) of WT and Akita age-matched mice were performed. Mice were dark-adapted overnight and anesthetized by i.p. injection using tribromoethanol. Pupils were then dilated with one drop of tropicamide ophthalmic solution (Akorn, Inc.). Full-field scotopic ERGs were recorded using the Tucker-Davis System Workstation (Tucker-Davis Technologies, Alachua, FL) for the real-time visualization of averaged a- and b-waves. BioSigRZ system was used for the quantification and further analysis.<sup>40,41</sup> Optical coherence tomography (OCT) was performed to visualize and compare the anatomic differences before and after JSH-23 treatment; Image-Guided OCT2 (Phoenix Technology Group, Pleasanton, CA) was used.<sup>42</sup> Spectral-domain OCTs on human subjects were obtained using a macular cube protocol on the Heidelberg SPECTRALIS (Heidelberg, Germany).

### Other Reagents and Antibodies

Chemicals and antibodies were purchased as indicated (eg, Sigma-Aldrich, Abcam, Cell Signaling Technology, or Santa Cruz Biotechnology). Details for the antibodies are as follows: inducible nitric oxide synthase (iNOS; ab15323) and NOD-like receptor family pyrin domain-containing 3 (NLRP3; ab214185) were purchased from Abcam (Cambridge, MA). Cyclooxygenase (COX)-2 (4842S), total NF-κB p65 (8242S), and phosphorylated NF-κB p65 (3033S) were purchased from Cell Signaling Technology (Danvers, MA). Intercellular adhesion

**Table 1** Nucleotide Sequence of Forward and Reverse Primers for the Genes Used in This Study

Gene	Forward sequence	Reverse sequence
<i>Rela</i> <sup>44</sup>	5' -GCCCGACCGCAGTATCC-3'	5' -GTCCCGCACTGTACCTG-3'
<i>Icam1</i> <sup>45</sup>	5' -TTCACACTGAATGCCAGCTC-3'	5' -GTCTGCTGAGACCCCTCTTG-3'
<i>Nos2</i> <sup>46</sup>	5' -CAGCTGGGCTGTACAAACCTT-3'	5' -CATTGGAAGTGAAGCGGTTTCG-3'
<i>Cox2</i> <sup>47</sup>	5' -CAGAACCGCATTGCCCTCTG-3'	5' -TTGTAACCTCTGGTCCTCATGTCTGA-3'
<i>Nlrp3</i> <sup>48</sup>	5' -CTTCTAGCTTCTGCCGTGGTCTCT-3'	5' -CGAAGCAGCATTGATGGGACA-3'
<i>Casp1</i> <sup>48</sup>	5' -GTACACGTCTTGCCCTCATTATCTG-3'	5' -TTTCACCTCTTTACCATCTCCAG-3'
<i>Il1b</i> <sup>48</sup>	5' -CAACCAACAAGTGATATTCTCCATG-3'	5' -GATCCACACTCTCCAGCTGCA-3'
<i>Cx43</i> <sup>49</sup>	5' -CCAAGGAGTTCCACCACTTTG-3'	5' -CCATGTCTGGGCACCTCTCT-3'
<i>Ocln</i> <sup>50</sup>	5' -AGACCCAAGAGCAGCCAAAG-3'	5' -GGAAGCGATGAAGCAGAAGG-3'
<i>Gapdh</i> <sup>48</sup>	5' -CATGGCTCCAAGGAGTAAGA-3'	5' -GAGGAGATGCTCAGTGTGG-3'

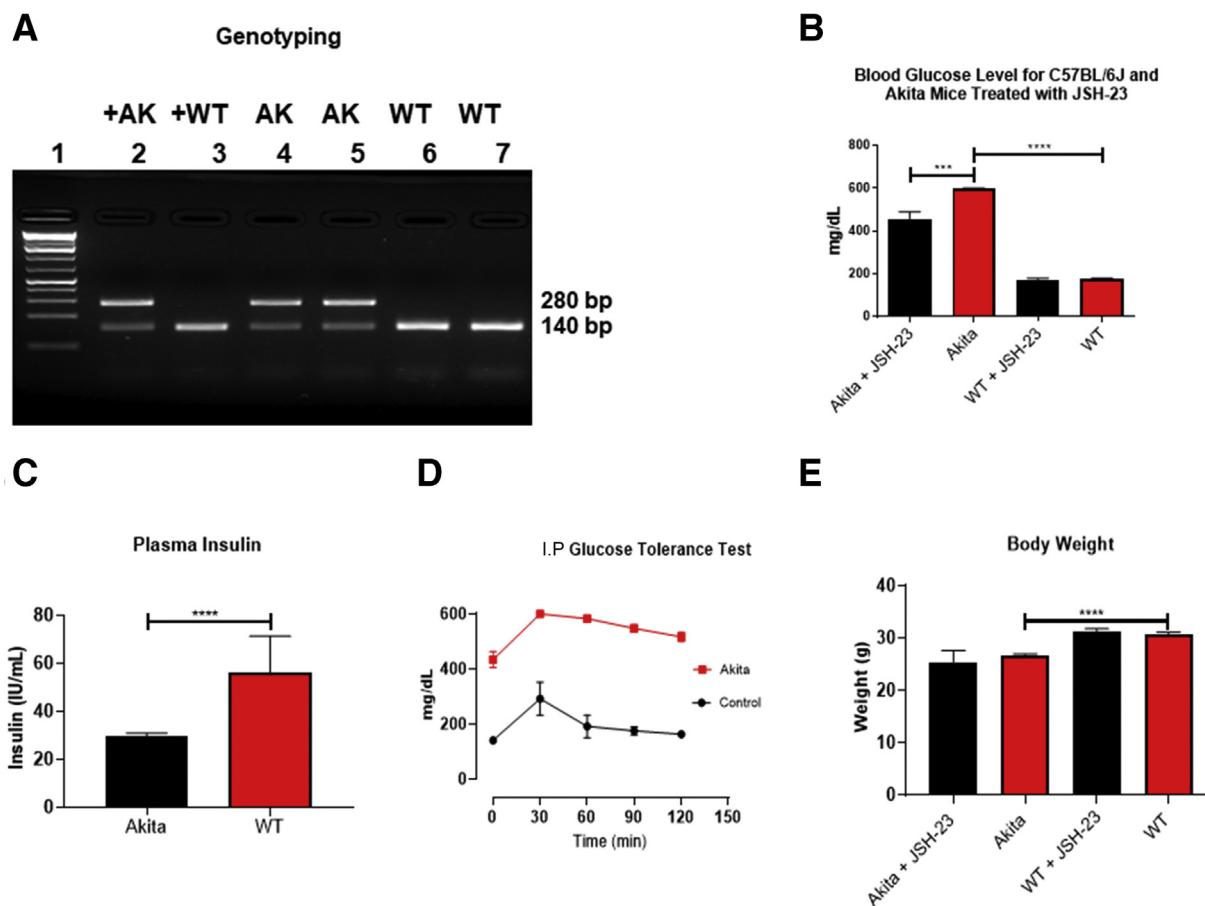


**Figure 1** Genotyping of mice strains and their glucose metabolic profile. **A:** Genotyping of Akita (AK) and wild-type (WT; C57BL/6J) mice. Lane 1 is a DNA size marker; lane 2 is a positive control for the Akita, and lane 3 represents a positive control for WT. Lanes 4 and 5 indicate Akita (*ins2<sup>Akita</sup>*) heterozygous mice exhibiting two bands: 280 and 140 bp, respectively, whereas WT mice show one 140-bp band in lanes 6 and 7. The +AK refers to Akita-positive control, whereas +WT refers to C57BL/6J genetic background positive control. **B:** Effect of the NF- $\kappa$ B inhibitor (alias JSH-23) on lowering the blood glucose levels in Akita mice compared with WT, measured in mg/dL. **C:** The plasma insulin level in Akita versus WT mice. **D:** The i.p. glucose tolerance test in Akita and WT. **E:** The body weights of Akita and the WT mice with or without JSH-23 treatment.  $n = 15$  (**B**);  $n = 19$  (**C** and **E**);  $n = 5$  (**D**). \*\*\* $P < 0.001$ , \*\*\*\* $P < 0.0001$ .

molecule-1 (ICAM-1; sc-107) was purchased from Santa Cruz Biotechnology (Dallas, TX). The secondary antibodies were also purchased from Santa Cruz Biotechnology [namely, rabbit anti-mouse (sc-358914), mouse anti-rabbit (sc-2357), and mouse anti-goat (sc-2354)]. Glyceraldehyde-3-phosphate dehydrogenase (GAPDH; MAB374) was purchased from EMD Millipore (Burlington, MA). All reagents and antibodies used for Western blotting were used following the manufacturers' recommended protocols.

### Analysis of the Key Inflammatory Molecules in the Diabetic Retina

Protein levels were detected via Western blot analyses. Retinae were separated from enucleated globes from euthanized mice. The retinal protein lysates were used immediately or snap frozen in liquid nitrogen and stored at  $-80^{\circ}\text{C}$  until further use. Proteins were extracted from the retinal samples via homogenizing in

radioimmunoprecipitation assay buffer (Boston Bio-Products, Worcester, MA) coupled with a cocktail of 1 mmol/L phenylmethylsulfonyl fluoride (Sigma, St. Louis, MO) and 1% protease inhibitors cocktail (Sigma). The samples were then sonicated with Sonifier 450 (Branson Ultrasonics, Danbury, CT). The homogenates were centrifuged at  $12,000 \times g$  for 15 minutes at  $4^{\circ}\text{C}$ , and the resultant supernatants were collected and stored at  $-80^{\circ}\text{C}$ . Bradford assay was used to estimate the total protein contents. Per sample, 40  $\mu\text{g}$  of total protein was resolved on a 10% SDS-PAGE and then transferred to polyvinylidene difluoride membrane. The polyvinylidene difluoride membranes were incubated with primary antibodies overnight and then with secondary antibodies the next day for 3 hours before visualization with ECL Luminata Forte (Millipore, Temecula, CA) via a Bio-Rad ChemiDoc system (BioRad Laboratories, Des Plaines, IL). Band intensities were normalized to GAPDH for all the target proteins analyzed, and their respective quantifications were performed through Image Lab Software (Bio-Rad, Hercules, CA).<sup>43</sup>



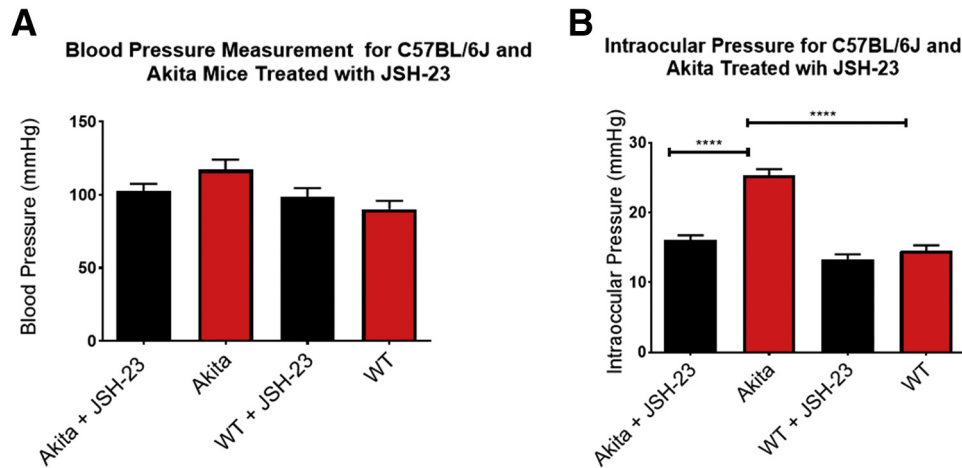


**Figure 2** Effect of JSH-23 on systemic blood pressure and intraocular pressure (IOP). **A:** There is no change in the systemic blood pressure in wild-type (WT) and Akita mice before and after treatment with JSH-23. **B:** However, IOP was higher in Akita mice, and could be lowered by the treatment with JSH-23. IOP is measured in mmHg.  $n = 8$  (A);  $n = 12$  (B). \*\*\*\* $P < 0.0001$ .

### Quantitative PCR

RNA was isolated with TRIzol reagent (Life Technologies, Carlsbad, CA) based on the manufacturer's instructions. Nanodrop-1000 (Thermo Scientific, Waltham, MA) was used to analyze RNA quantification and purity. ImProm-II Reverse Transcription System (A300; Promega, Madison, WI) was used to reverse transcribe the total RNA into cDNA per manufacturer's instructions. Quantitative PCR was performed for different transcripts (*RelA*, *ICMA1*, *iNOS*, *COX-2*, *NLRP3*, *Casp1*, *IL-1B*, *Cx43*, *Occludin*, and *GAPDH*). The final reaction included 10  $\mu$ L of nuclease-free water, 8  $\mu$ L of Bullseye EvaGreen qPCR Mastermix (BEQPCR-S; MIDSCI, Valley Park, MO), 50 pmol of forward and reverse primers in 1  $\mu$ L, and 1  $\mu$ L of cDNA (Table 1<sup>44–50</sup>). Data were normalized with the housekeeping gene *GAPDH*.<sup>51</sup>

### The Light-Dark Chamber Movement Test

Individual animals were subjected to the light-dark box test. The PACS Shuttle Box Version 3.40 (Passive/Active Avoidance Chamber System-30; Columbus Instruments, Columbus, OH) was set up in experiment mode as passive avoidance, with unified computing system grid intensity (amperes), 0; exploration duration, 30 seconds; maximal trial duration, 5 minutes; conditioned stimulus light intensity, 10 V; and unified computing system grid duration, 2 seconds. After 30 seconds of exploration, the light flickered on. The time taken for the mouse to transfer from the light chamber to the dark was measured.<sup>52</sup>

### Human FA and OCT Measurements

Images of FA from a normal and a diabetic human eye are provided for comparison with Akita mice. Fundus FA was performed as part of routine clinical care of human patients

using the Heidelberg SPECTRALIS fundus camera after injecting sodium fluorescein 10% intravenously (Heidelberg Engineering, Heidelberg, Germany). The diabetic and the nondiabetic persons underwent a full dilated eye examination and spectral-domain OCT (Zeiss Cirrus HD-OCT 5000; Carl Zeiss Meditec, Inc., Dublin, CA) of a  $6 \times 6$ -mm area of the macula in their eyes. The images were analyzed and classified as either normal or having diabetic macular edema.

### Statistical Analysis

All values are reported as means  $\pm$  SEM. One-way analysis of variance was used to analyze the differences between the groups, including the Tukey post hoc analysis for group comparisons. The tests were performed with  $P < 0.05$ , and the total number of mice, at least  $n = 5$  to 20, was subjected to experimentations from each group. GraphPad Prism version 8.3.0 (GraphPad Software, San Diego, CA) was used during analyses.

## Results

### Confirmation of Ins2<sup>Akita</sup> Mutation in the Expanded Mouse Colony and Determination of the Effect of JSH-23 on Glucose Metabolism

Tail-clip DNA samples were analyzed using PCR with specific primers to determine the genotype of newly bred pups. The mutated version of the insulin gene exhibited two discrete bands: 280 and 140 bp, representing Akita mice's heterozygous status, whereas WT mice showed one 140-bp band (Figure 1A).<sup>31</sup> Akita mice's blood glucose levels were significantly higher than those of WT mice ( $P < 0.0001$ ;  $n = 15$  per group), and JSH-23 decreased these levels in Akita mice ( $P < 0.0001$ ) (Figure 1B). Akita mice displayed significantly lower plasma insulin levels than in WT mice

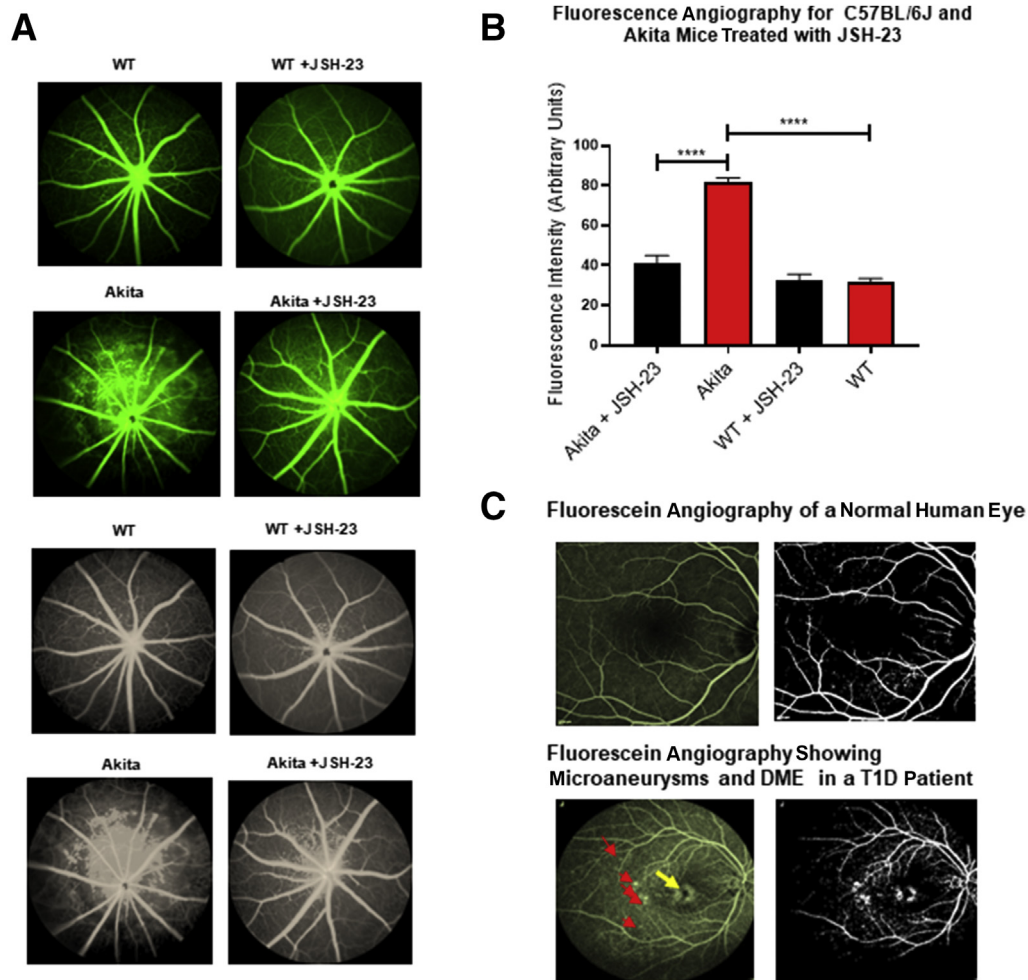


**Figure 3** Anti-inflammatory effects of JSH-23 on retinal vasculature. **A:** Fluorescein angiography (FA) in wild-type (WT) and Akita mice treated with JSH-23 compared with untreated mice. **B:** Quantitative analysis of retinal blood vessel permeability, as shown in **A**, using the ImageJ2 program; the anti-inflammatory effect is evident after treatment in the Akita mice. **C:** Comparison of a normal human eye with that of the late-phase FA of the right eye in a patient with type 1 diabetes (T1D), showing microaneurysms and diabetic macular edema (DME). The **red arrows** are microaneurysms, whereas the **yellow arrow** shows the macular edema.  $n = 6$  (**B**). \*\*\*\* $P < 0.0001$ .

( $P < 0.0001$ ;  $n = 19$  per group) (Figure 1C). As expected, the i.p. glucose tolerance test showed high glucose levels in Akita mice than in WT mice. Furthermore, i.p. glucose tolerance test also indicated that the Akita strain was unable to lower its blood glucose levels ( $P < 0.0090$ ;  $n = 5$  per group) (Figure 1D). The body weights were measured before and after JSH-23 treatment. Akita mice body weights were significantly lower than age-matched WT control mice; JSH-23 had no effect on body weights (Figure 1E). This could be a result of a decrease in their lean mass compared with WT control littermates, most likely as a function of age.<sup>53</sup>

### Monitoring of Blood Pressure and IOP

Systemic blood pressure and IOP were evaluated before and after treatment with JSH-23. JSH-23 is known to increase blood pressure in hypertriglyceridemic rats.<sup>54</sup> Therefore, it was imperative to determine whether JSH-23 alters the

systemic blood pressure of the mice. Treated and untreated mice were subjected to a noninvasive tail-cuff method for recording their blood pressure. None of the mice acquired a statistically significant change in systemic blood pressure ( $n = 8$  per group) (Figure 2A); however, IOP was higher in Akita mice than in age-matched WT control mice ( $P < 0.0001$ ;  $n = 12$  per group). Intervention with JSH-23 decreased the elevated IOP significantly in the Akita mice group ( $P < 0.0001$ ) (Figure 2B).

### Assessment of Retinal Vasculature by Angiography and Fundoscopy

Retinal vascular leakage is exacerbated by inflammation, making inflammation a key component in DR pathology. FA was employed to study the anti-inflammatory effects of JSH-23 on the retinal vasculature *in vivo*.<sup>27</sup> Akita mice's retinal vasculature indicated microaneurysms and increased vascular permeability ( $P < 0.0001$ ;  $n = 6$  per group). JSH-

23 treatment prevented vascular impairments, depicting low vascular permeability in this mouse strain ( $P < 0.0001$ ) (Figure 3, A and B). FA images taken from a healthy human and a patient with T1D eyes are shown for comparison (Figure 3C). The optic nerve is eccentric from the center of the fundus in humans. DR leakage occurs predominantly around the fovea in humans, indicating the center of macula. Multiple microaneurysms were observed in both human and mouse eyes.

### Evaluation of *In Vivo* ERG and OCT

Full-field scotopic ERGs evaluated functional changes in the retina of WT and Akita mice. BioSigRZ system was used for real-time visualization of the averaged A- and B-waves. Akita mice demonstrated widened but truncated A- and B-waves in contrast to the sharp A- and B-waves in WT mice (Figure 4A). The A-wave amplitude in the retinae of Akita mice decreased ( $P < 0.0001$ ;  $n = 6$  per group); however, the treatment with JSH-23 prevented a decrease in the A-wave amplitude in Akita mice ( $P < 0.0001$ )

(Figure 4B). The B-wave amplitude in Akita mice also decreased ( $P < 0.0001$ ;  $n = 6$  per group); JSH-23 treatment prevent this decrease in B-wave amplitude in Akita mice ( $P < 0.0001$ ) (Figure 4C).

The retinal structural integrity was evaluated with real-time, image-guided optical OCT in Akita mice. It displayed hyporeflective retinal lucency and abnormal thickening of membrana limitans interna, inner nervous stratum opticum, and the ganglionic layer. Also, there was a focal discontinuity in the retinal pigment epithelium captured by Micron-IV OCT2 in Akita mice (Figure 5A). These alterations were prevented by JSH-23 treatment (Figure 5B). Figure 5C depicts the healthy eye versus a diabetic eye from a T1D patient, highlighting diabetic macular edema.

### Treatment with JSH-23 Diminishes Key Inflammatory Molecules in the Diabetic Retina

To examine the effects of NF- $\kappa$ B inhibition in mice retinae, Western blotting and quantitative PCR analyses of the retinal lysates from JSH-23-treated and untreated mice were

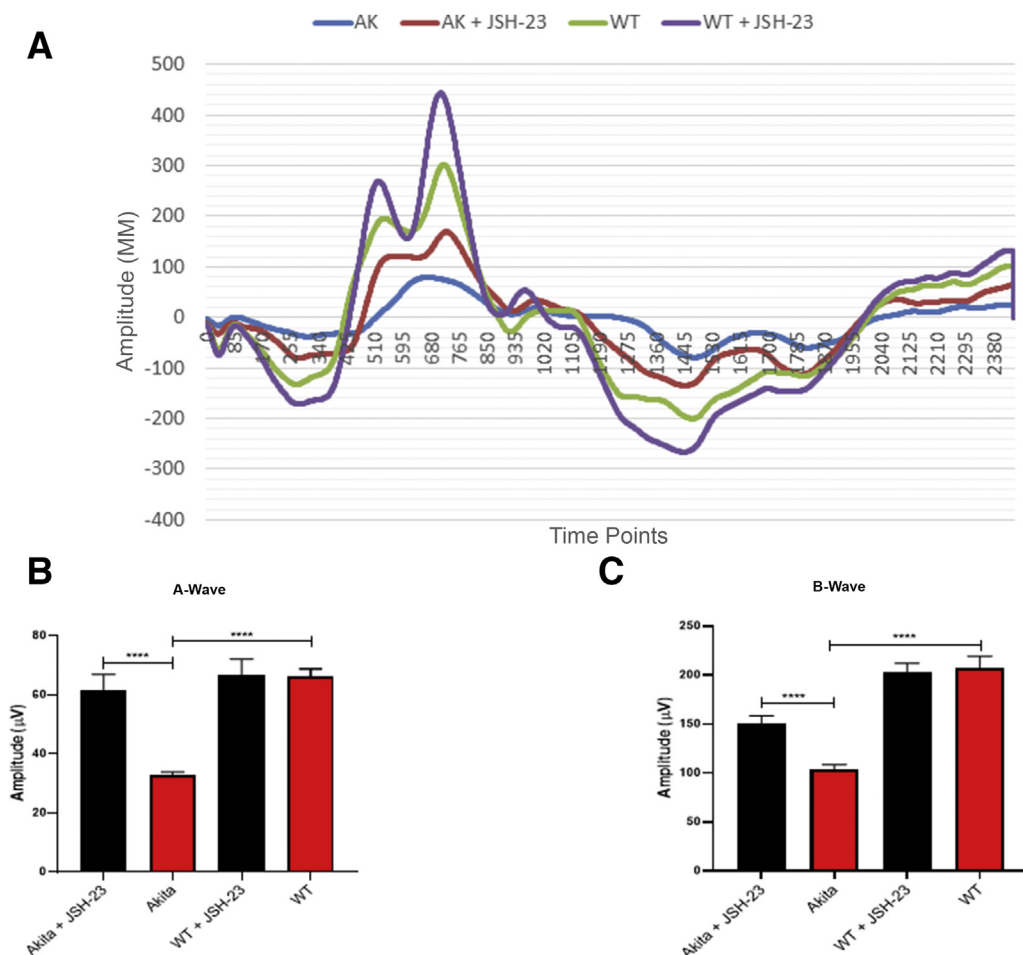


**Figure 4** **A:** Electrorretinograms (ERGs) of wild-type (WT) and Akita (AK) mice treated or untreated with JSH-23. Quantitative depictions of the ERG patterns when superimposed on top of each other mark the relative differences in amplitudes. **B** and **C:** Amplitudes of A-wave (**B**) and B-wave (**C**) in the retinae of Akita and WT mice with or without JSH-23  $n = 6$  (**B** and **C**). \*\*\*\* $P < 0.0001$ .

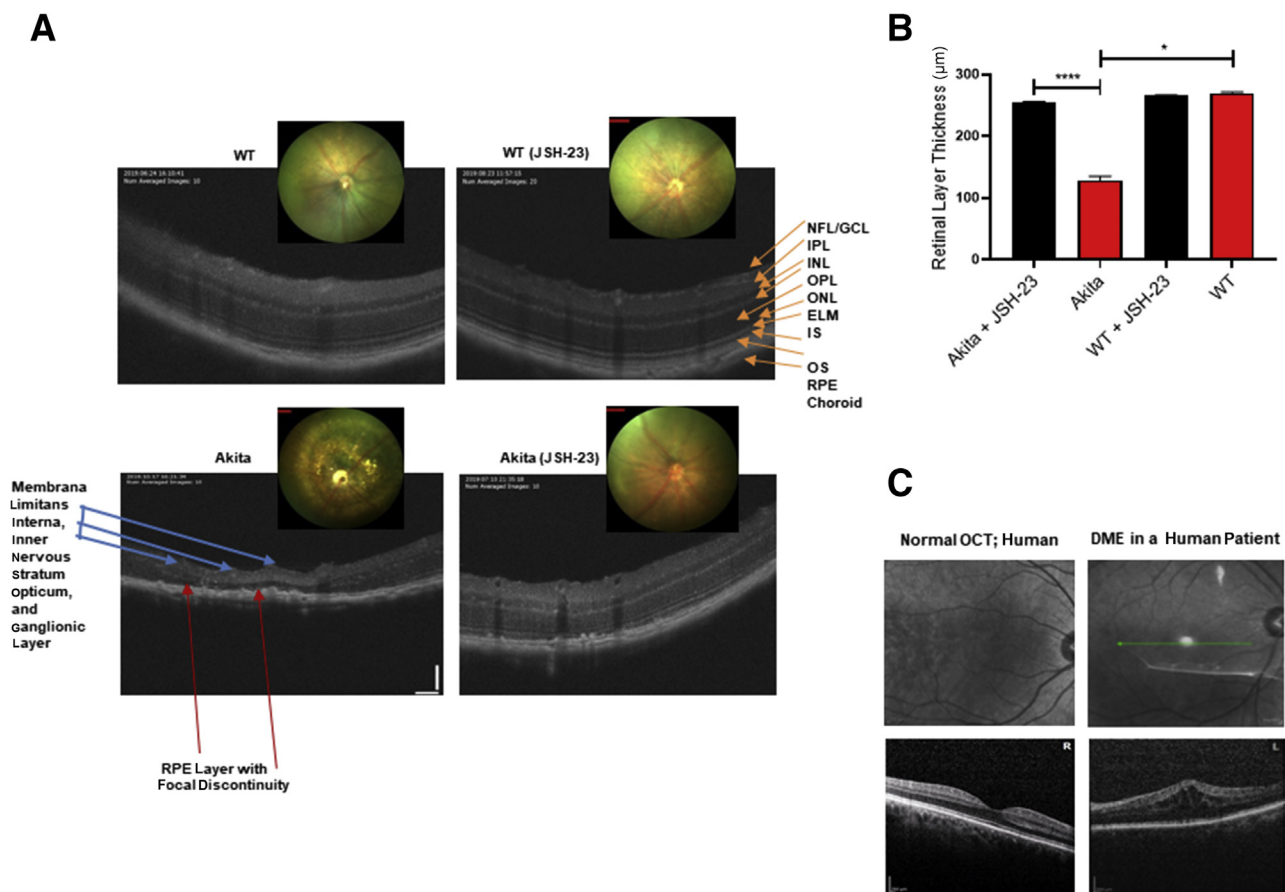


**Figure 5** **A:** Optical coherence tomography (OCT) in Akita and wild-type (WT) mice treated with JSH-23. The OCT measurements of the central retinae indicate that JSH-23 treatment was able to prevent the degradation of retinal layers. Changes in the retinal layers of Akita mice, such as discontinuity in the retinal pigment epithelium (RPE) and notable alterations, are indicated by blue and red arrows. **B:** Quantitative assessment of the retinal layer thickness in WT and Akita with or without JSH-23 treatment, showing the beneficial effects of JSH-23 in Akita toward restoration of retinal integrity. **C:** A spectral-domain OCT through patient's fovea (shown earlier in Figure 3C) for comparison. The green arrow represents the location of OCT measurement.  $n = 6$  (**B**).  $*P < 0.05$ ,  $****P < 0.0001$ . Scale bars = 100  $\mu\text{m}$  (**A**). DME, diabetic macular edema. ELM, external limiting membrane; GCL, ganglion cell layer; IP, inner plexiform layer; IS, inner segment; NFL, nerve fiber layer; ON, outer nuclear layer; OPL, outer plexiform layer; OS, outer segment; RPE, retinal pigment epithelium.

examined for the ratio of phosphorylated/total protein levels of NF- $\kappa$ B p65 and RelA gene expression. The ratio was significantly higher in Akita compared with WT mice ( $P < 0.0005$ ;  $n = 5$  per group) (Figure 6, A and B). JSH-23 treatment significantly decreased this ratio in Akita mice ( $P < 0.0016$ ). RelA gene expression was higher in the retinae of Akita mice ( $P < 0.0001$ ;  $n = 5$  per group) (Figure 6C), which was decreased with JSH-23 treatment ( $P < 0.0002$ ;  $n = 5$  per group). Similarly, ICAM-1 protein levels ( $P < 0.0218$ ;  $n = 6$  per group) and gene expression ( $P < 0.0003$ ;  $n = 5$  per group) were elevated in the retinae of Akita mice; JSH-23 treatment decreased both the protein levels ( $P < 0.0028$ ) and gene expression ( $P < 0.0001$ ;  $n = 5$  per group) (Figure 7, A and B, and Figure 8A). The iNOS protein levels ( $P < 0.0001$ ;  $n = 6$  per group) and gene expression ( $P < 0.0012$ ;  $n = 5$  per group) were also higher in the retinae of Akita mice. JSH-23 decreased both the protein levels ( $P < 0.0001$ ;  $n = 6$  per group) and the gene expression

( $P < 0.0031$ ;  $n = 5$  per group) (Figure 7, A and B, and Figure 8B). In addition, COX-2 protein levels ( $P < 0.0001$ ;  $n = 6$  per group) and gene expression ( $P < 0.0004$ ;  $n = 5$  per group) were higher in the retinae of Akita mice. JSH-23 treatment decreased both the levels of COX-2 protein ( $P < 0.0001$ ;  $n = 6$  per group) and gene expression ( $P < 0.0001$ ;  $n = 5$  per group) (Figures 7C and 8C).

NLRP3 protein levels ( $P < 0.0180$ ;  $n = 6$  per group) and gene expression ( $P < 0.0025$ ;  $n = 6$  per group) were higher in the retinae of Akita mice. JSH-23 treatment decreased both the NLRP3 protein levels ( $P < 0.0003$ ;  $n = 6$  per group) and gene expression ( $P < 0.0003$ ;  $n = 6$  per group) (Figure 9, A–C). The genes for *casp1* ( $P < 0.0001$ ;  $n = 6$  per group) and *IL-1B* ( $P < 0.0001$ ;  $n = 6$  per group) had increased expression in the retinae of Akita mice. JSH-23 treatment decreased the expression of both *casp1* ( $P < 0.0001$ ;  $n = 6$  per group) and *IL-1B* ( $P < 0.0001$ ;  $n = 6$  per group) (Figure 9, D and E).



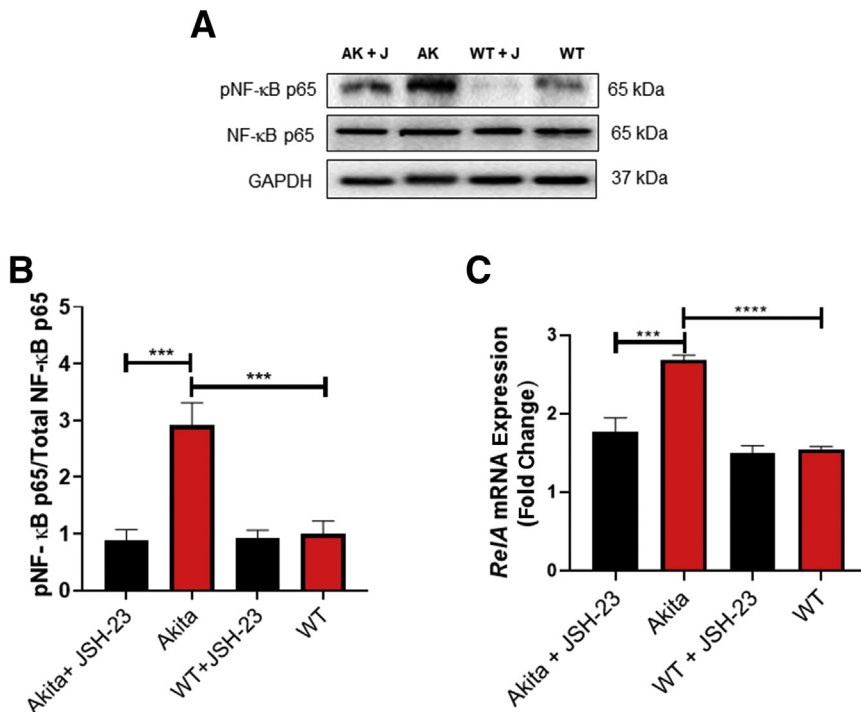


**Figure 6** **A:** Western blotting depicting protein levels of key inflammatory molecules in wild-type (WT) and Akita (AK) mice treated with JSH-23 (J). Immunoblotting image of the total and phosphorylated NF- $\kappa$ B p65 protein in AK + J, AK, and WT + J mice. **B:** Quantification of the protein levels of phosphorylated NF- $\kappa$ B (pNF- $\kappa$ B) p65 with respect to total NF- $\kappa$ B p65. Akita mice have elevated levels of phosphorylated version of the NF- $\kappa$ B protein, and JSH-23 decreased their respective levels after treatment. **C:** RelA gene expression in the retinae of Akita and WT mice treated or untreated with JSH-23. The gene expression of *RelA* was higher in Akita compared with WT mice.  $n = 5$  (**B** and **C**). \*\*\* $P < 0.001$ , \*\*\*\* $P < 0.0001$ . GAPDH, glyceraldehyde-3-phosphate dehydrogenase.

### JSH-23 Maintained Integrity of the Tight and Gap Junctions along with Barrier Function Proteins in Diabetic Retina

Hyperglycemia-induced down-regulation of connexin-43 severely affects gap junction intercellular communication in blood vessels. Therefore, it contributes to the breakdown of endothelial tight junctions in DR.<sup>55</sup> Occludin and connexin-43 protein levels and their gene expression were analyzed by employing Western blotting and real-time PCR. Connexin-43 protein levels ( $P < 0.0165$ ;  $n = 5$  per group) and gene expression ( $P < 0.0003$ ;  $n = 5$  per group) were significantly decreased in the retina of Akita. JSH-23-treatment maintained connexin-43 protein levels ( $P < 0.0006$ ;  $n = 5$  per group) and gene expression ( $P < 0.0237$ ;  $n = 5$  per group) in the retinae of Akita mice (Figure 10, A, B, and D). Similarly, occludin protein levels ( $P < 0.0068$ ;  $n = 5$  per group) and gene expression ( $P < 0.0073$ ;  $n = 5$  per group) were significantly decreased in the retinae of Akita mice. JSH-23 prevented the degradation of the protein ( $P < 0.0071$ ;  $n = 5$  per group) and gene expression ( $P < 0.0060$ ;  $n = 5$  per group) of occludin in the Akita mice (Figure 10, A, C, and E).

### Evaluation of Vision-Guided Behavior in JSH-23-Treated Mice

The mice were evaluated for their vision-guided behavior by employing a light-dark chamber analysis. It took Akita mice significantly longer to move from the light chamber

into the dark chamber ( $P < 0.0001$ ;  $n = 8$  per group) relative to WT mice. However, JSH-23 significantly decreased the time Akita mice took to move from the light chamber to the dark chamber ( $P < 0.0477$ ;  $n = 8$  per group) (Figure 11).

## Discussion

T1D leads to a predisposition to long-term medical complications, including blindness. Twenty years after diagnosis, approximately 98% of T1D patients exhibit DR pathology.<sup>56</sup> As a result, DR is becoming a serious medical problem globally. Currently there is no cure for DR. Early detection and intervention can reduce the risk, but vision loss can be irreversible for many. Research has identified several options to manage DR symptoms, but not all T1D patients benefit from them. In this study, mitigating inflammation via blocking NF- $\kappa$ B activity demonstrated that specific targeting of inflammation over a longer period could help prevent retinal complications in the diabetic eye. Thus, the findings highlight that targeted intervention could help mitigate retinopathy. Overall, JSH-23 alleviated retinovascular remodeling, including permeability, indicating that inhibition of inflammation via NF- $\kappa$ B helps protect the diabetic retina.<sup>23,25–27,57–62</sup>

Activation of NF- $\kappa$ B and its subsequent nuclear translocation can be separated from other biological processes, thus allowing an opportunity to test its targeting, thereby inhibiting its transcriptional activity. The current study used a T1D model that shows degenerative changes in the

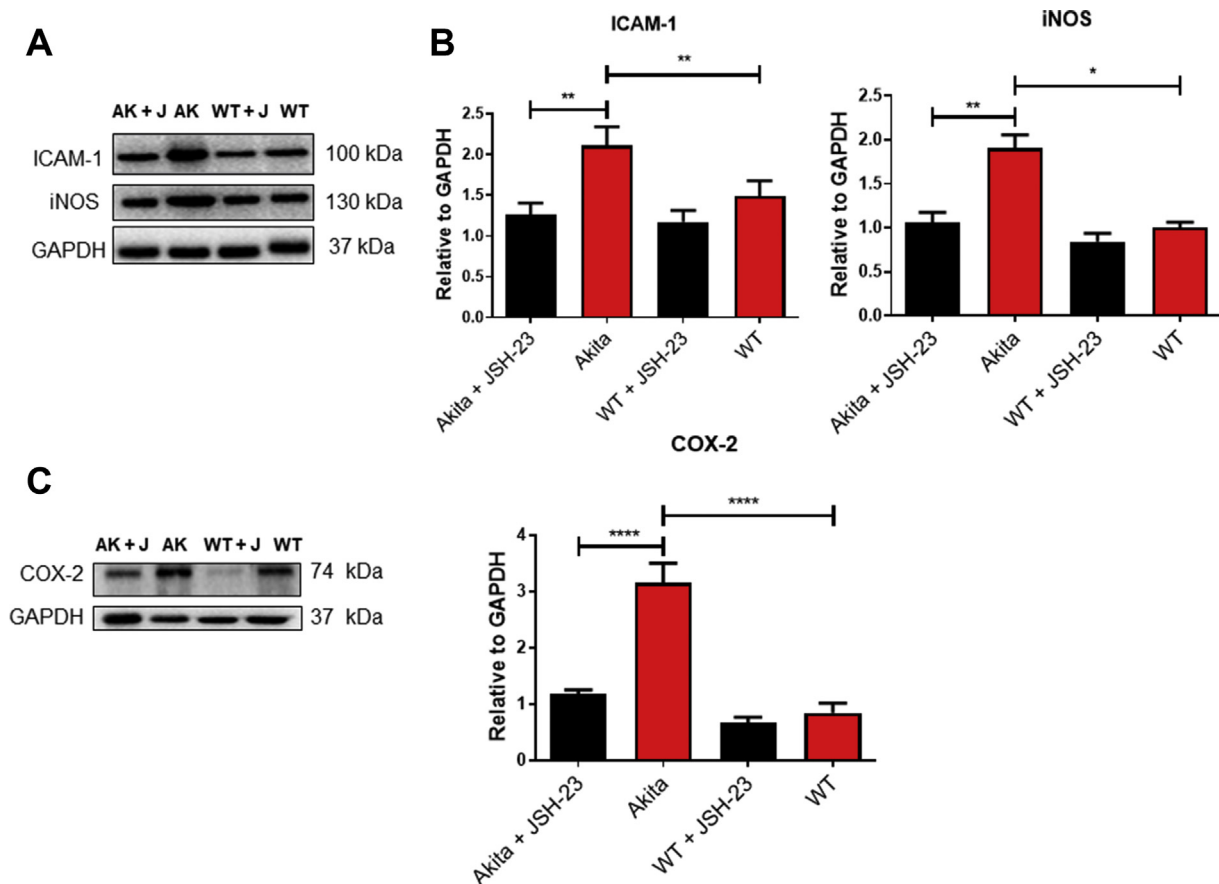


**Figure 7** Immunoblotting of intercellular adhesion molecule (ICAM)-1, inducible nitric oxide synthase (iNOS), and cyclooxygenase (COX)-2 proteins. **A:** Representative immunoblot showing higher ICAM-1 and iNOS protein levels in Akita (AK) mice than in wild-type (WT) mice. **B:** Quantitation of ICAM-1 and iNOS proteins and their lowering by JSH-23 (J) treatment **C:** Quantification of COX-2 protein and its lowering after JSH-23 treatment.  $n = 6$  (**B** and **C**). \* $P < 0.05$ , \*\* $P < 0.01$ , and \*\*\*\* $P < 0.0001$ . GAPDH, glyceraldehyde-3-phosphate dehydrogenase.

retinal architecture, including its vasculature.<sup>63</sup> To test this hypothesis, WT and Akita (Ins<sup>2Akita</sup>) mice were treated with JSH-23 for 4 weeks continuously. Several disease indicators and parameters (eg, IOP, blood pressure, blood glucose levels, retinal structure, visual function, and inflammatory mediators) were evaluated, including vision-guided behavioral analysis. FA, OCT, and ERG were employed to assess structural and functional aspects of the retina. JSH-23 significantly decreased retinal vasculopathy in the retinæ of Akita mice. FA showed that JSH-23 prevented an increase in vascular leakage in Akita mice. Interestingly, 4 weeks of intervention with JSH-23 was sufficient to avoid any change in retinal thickness after >20 weeks of hyperglycemia. It is imperative to analyze whether the retinal thickness/biomass lost can be recovered after JSH-23 intervention in the Akita mice. The OCT measurements of the central retinæ showed that JSH-23 treatment was able to prevent the degradation of retinal layers in Akita mice. It would be of great significance to analyze further the effect(s) of JSH-23 on retinal degeneration phenotype in the aged/old mice. However, in this study, the decrease in pathologic

changes in the retinæ of Akita mice was appreciable for potentially delaying the further retinal pathology, the onset of proliferative diabetic retinopathy, and vision loss in these mice (Figure 3, A and B, Figure 4, A and B, and Figure 5, A and B).

Inflammation in the retinal vasculature was significantly diminished. Key inflammatory mediators (eg, ICAM-1, iNOS, and COX-2) were analyzed in Akita mice retina. NF- $\kappa$ B p65 or RelA contain the conserved Rel homology domain, which plays a role in dimerization and DNA binding. RelA generally heterodimerizes with NF- $\kappa$ B p50 subunits and contains the transactivating domains. The transactivating domain functions in the transcriptional activity of the dimers. Once activated, NF- $\kappa$ B undergoes various modifications, including acetylation and methylation. However, phosphorylation is critical in regulating NF- $\kappa$ B activity. Although NF- $\kappa$ B phosphorylation does not act as an on or off switch, the site phosphorylation regulates certain NF- $\kappa$ B activity.<sup>64</sup> RelA is known to be phosphorylated in many places (eg, serine 205, 276, and 281 in the Rel homology domain). These sites phosphorylate via various kinases, such as protein kinase A.<sup>65</sup>

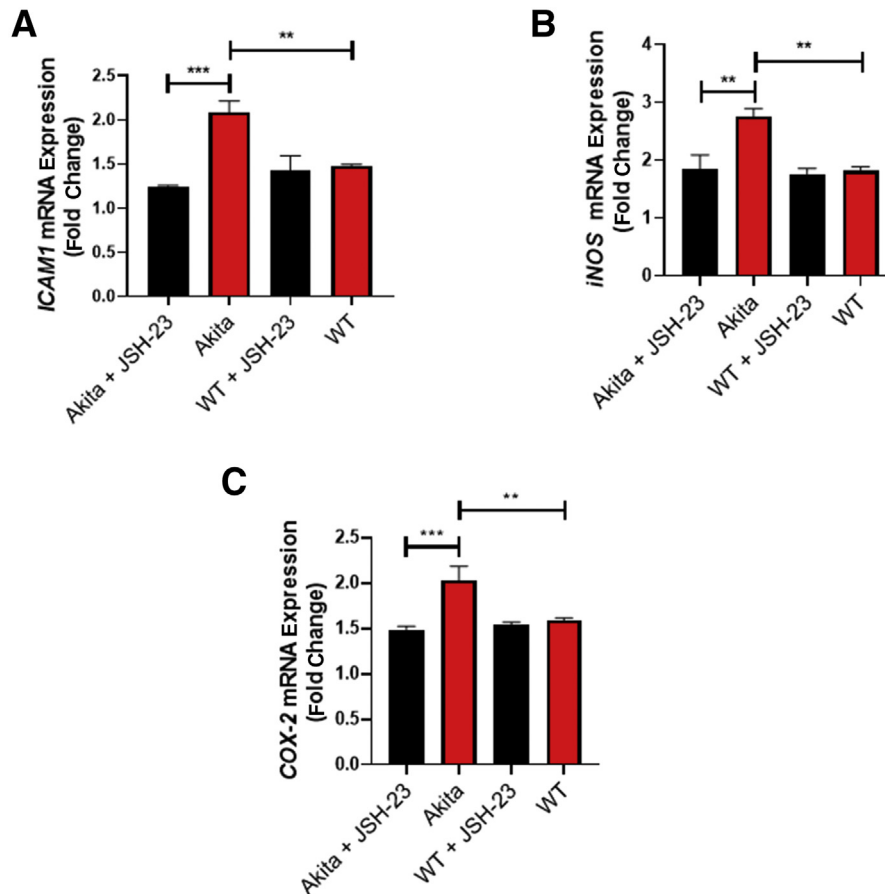


**Figure 8** Gene expression profiling for *ICAM-1* (A), *iNOS* (B), and *COX-2* (C) markers in Akita mice, corroborating the findings of the respective proteins in the Akita (Figure 7) after JSH-23 treatment.  $n = 5$  (A–C). \*\* $P < 0.01$ , \*\*\* $P < 0.001$ . WT, wild type.

JSH-23 inhibits the nuclear translocation of NF- $\kappa$ B p65/p50, thus inhibiting the most prevalent heterodimers of NF- $\kappa$ B inflammatory response. Kumar et al<sup>13</sup> showed that JSH-23 inhibits nuclear translocation of NF- $\kappa$ B p65/p50 in streptozotocin-induced diabetic rats at 3 mg/kg after 2 weeks of oral administration. Chi et al<sup>66</sup> showed that JSH-23 injected into the vitreous inhibited phosphorylated NF- $\kappa$ B p65 and activation of the NLRP3 inflammasome in a glaucoma mouse model. The study showed that the ratio of phosphorylated NF- $\kappa$ B p65/total NF- $\kappa$ B p65 was significantly reduced in the retina of Akita mice, potentially indicating that JSH-23 is a selective and specific inhibitor. Mattioli et al<sup>67</sup> showed that phosphorylation of NF- $\kappa$ B p65 at serine 536 in the cytoplasm inhibits nuclear translocation, the exact mechanism of which (whether or not it is site-specific) is yet to be. It is important to analyze that ratio through a nuclear extract of the retina treated with JSH-23. Currently, the JSH-23 effect is typically analyzed via nuclear extract, like in Kumar et al,<sup>13</sup> or cytoplasmic extract, like in Chi et al.<sup>66</sup>

Treatment with JSH-23 unexpectedly decreased blood glucose levels in Akita however, it could be due to increased insulin sensitivity in Akita mice. A decrease in inflammation increases insulin sensitivity. Hyperglycemia activates NF-

$\kappa$ B, increasing insulin resistance, and chemical or genetic inhibition improves insulin resistance.<sup>68</sup> This study also demonstrated that treatment with JSH-23 can decrease IOP in Akita mice.

Multiple demographic studies have indicated an increase in IOP in diabetic patients versus nondiabetic patients. This increase in IOP is independent of open-angle glaucoma; however, the mechanism has not yet been elucidated. Glycosylated hemoglobin can cause an osmotic gradient that shifts fluid between plasma and the intraocular, thus elevating the IOP. A Japanese study found a significant correlation between IOP and glycosylated hemoglobin levels in patients with DR.<sup>69</sup> A Chinese population study also found an association of glycosylated hemoglobin with high IOP (>21 mmHg).<sup>70</sup> Additionally a demographic study in Singapore found an association showing elevated IOP. Even after accounting for the difference in central corneal thickness, which is higher in diabetic individuals, the IOP increase was independent of glaucoma development. The current study showed no change in the systemic blood pressure of mice. One of the significant findings of this work is that mitigating inflammation most likely helped improve Akita's vision, scored via the vision-guided behavioral test.

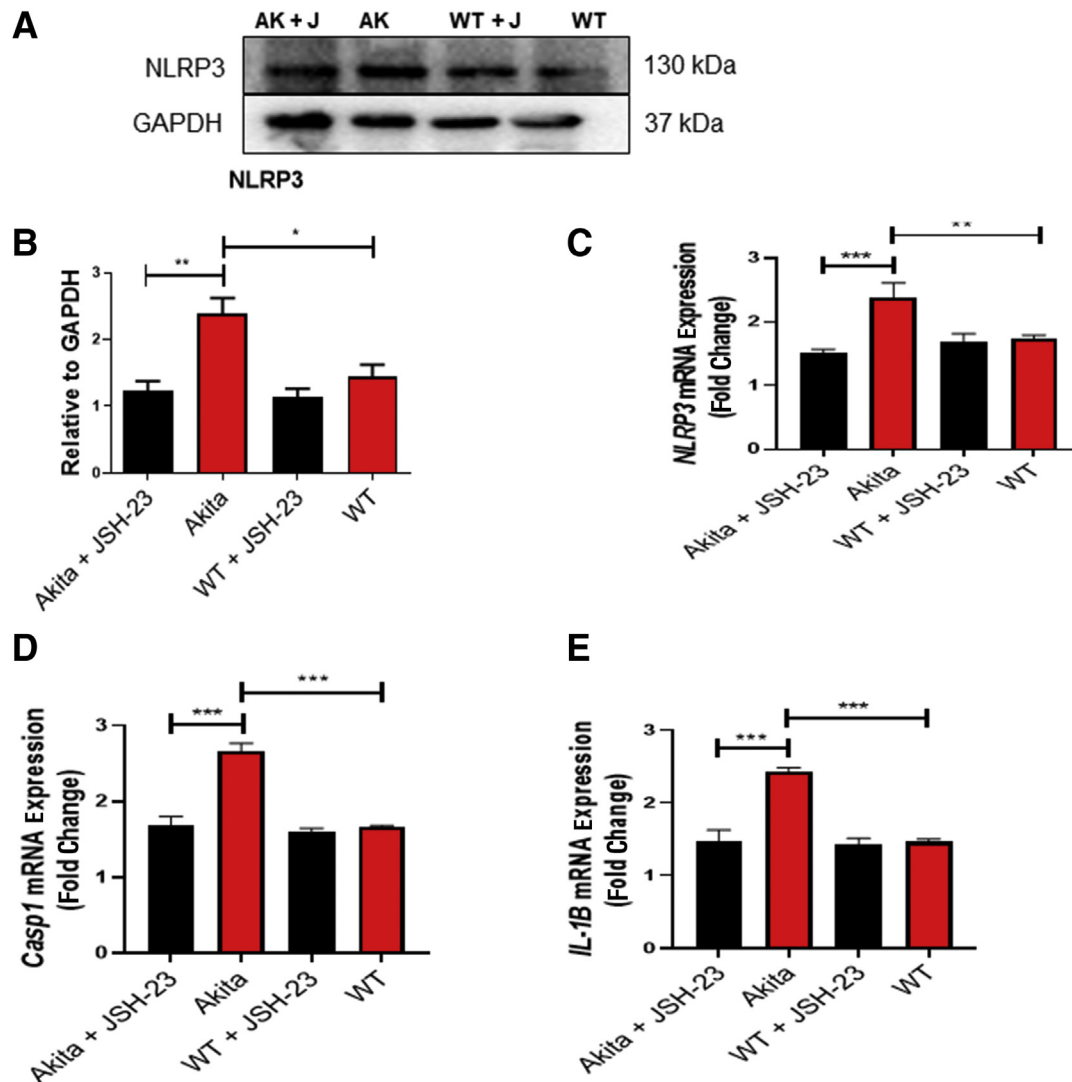


**Figure 9** Immunoblotting and gene expression analyses. Protein levels of the NOD-like receptor family pyrin domain-containing 3 (NLRP3; **A**), its quantitation (**B**), and gene expression analyses of *NLRP3* (**C**), *Casp1* (**D**), and *IL-1β* (**E**), reiterating heightened levels in Akita (AK) mice. Their respective levels decreased significantly after treatment with JSH-23 (J).  $n = 6$  (**B–E**). \* $P < 0.05$ , \*\* $P < 0.01$ , and \*\*\* $P < 0.001$ . GAPDH, glyceraldehyde-3-phosphate dehydrogenase; WT, wild type.

This data set indicates that controlling inflammation can potentially help decrease retinal inflammatory insults, thereby improving structural and functional attributes of the diabetic retina.

NF-κB regulates the survival, activation, and differentiation of immune cells. It has also been implicated in other processes, including synaptic plasticity.<sup>10,71,72</sup> Some of the essential targets of NF-κB include iNOS, ICAMs, and growth factors. Many NF-κB targets are inflammatory mediators associated with the development of retinopathy in diabetic patients. Notably, iNOS-mediated nitric oxide production from L-arginine primarily mediates inflammation. Physiological production of nitric oxide is generated by the action of neuronal and endothelial synthases.<sup>73</sup> Although iNOS is not expressed in most resting cells, it has high expression in activated immune cells.<sup>74</sup> Activated

NF-κB induces transcription of iNOS because increased iNOS levels have been reported in the retinae of diabetic animals.<sup>10</sup> Increase in iNOS is associated with apoptosis, leukostasis, and BRB breakdown.<sup>75</sup>

Studies on retinal cells exposed to high glucose concentrations demonstrate that nitric oxide (particularly iNOS-generated) increases other inflammatory mediators, such as COX-2.<sup>23</sup> Cyclooxygenases mediate eicosanoid synthesis. Their primary function is to generate prostaglandins. COX-1 maintains the physiological production of eicosanoids.<sup>76</sup> COX-2 remains absent from most tissues and its expression increases in the presence of lipopolysaccharides and proinflammatory cytokines. COX-2 exhibits higher expression in monocytes, macrophages, and endothelial cells.<sup>76</sup> NF-κB activation up-regulates COX-2 gene expression in retinal cells; and high COX-2



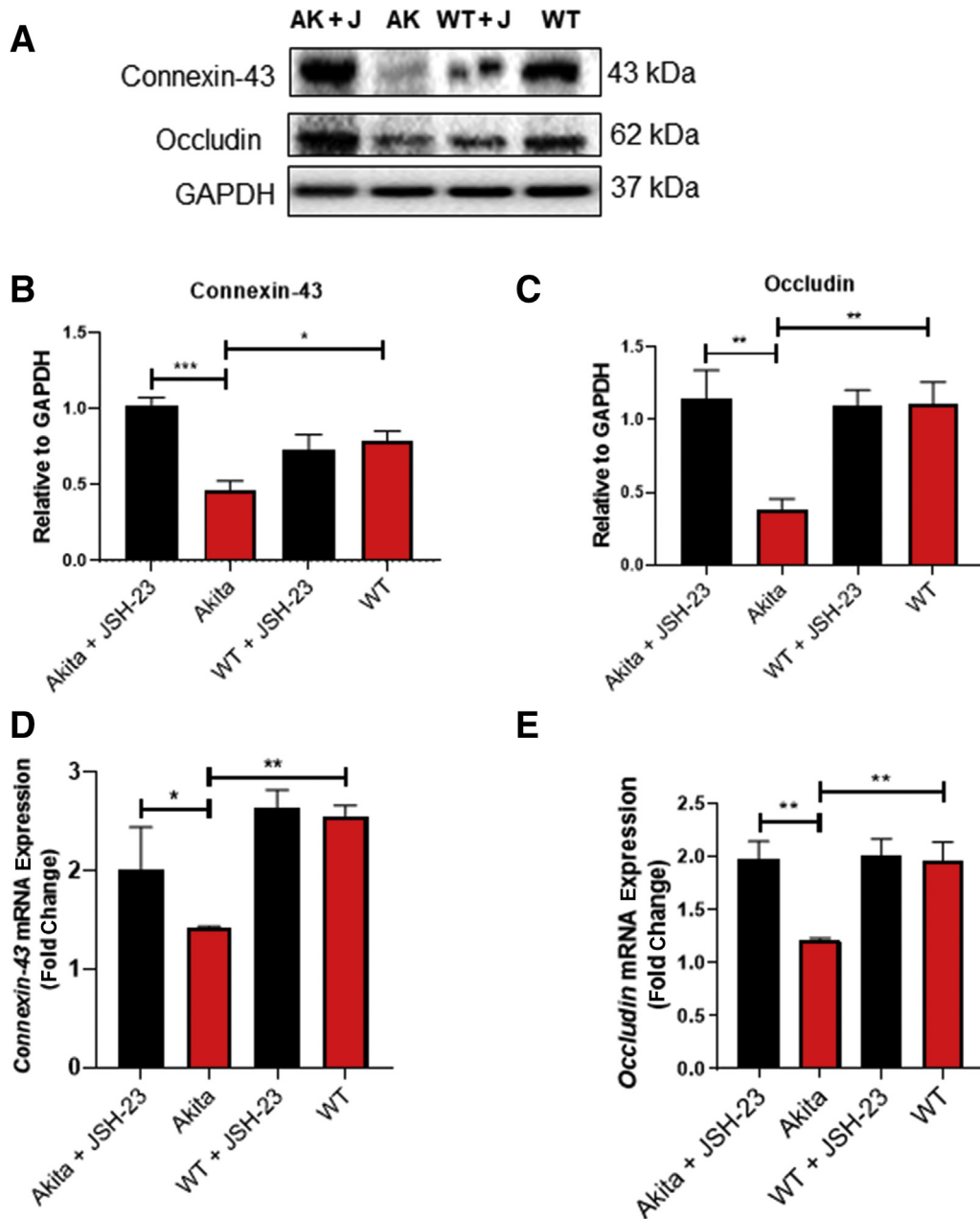


**Figure 10** Connexin-43 and occludin protein levels and their gene expression analyses in wild-type (WT) mice and Akita (AK) mice treated with JSH-23 (J). **A:** Immunoblotting image of connexin-43 and occludin. **B:** Connexin-43 protein levels in Akita mice and WT mice treated with or without JSH-23. **C:** Occludin protein levels in Akita mice and WT mice treated with or without JSH-23. **D:** *Connexin-43* gene expression in Akita mice and WT mice treated with or without JSH-23. **E:** *Occludin* gene expression in Akita mice and WT mice treated with or without JSH-23.  $n = 5$  (**B–E**). \* $P < 0.05$ , \*\* $P < 0.01$ , and \*\*\* $P < 0.001$ . GAPDH, glyceraldehyde-3-phosphate dehydrogenase.

expression is associated with BRB breakdown.<sup>77,78</sup> *COX-2* expression increased in Akita mice retinas.<sup>79</sup> Other inflammatory mediators regulated by NF- $\kappa$ B and with increased expression in the diabetic retinas are ICAMs, particularly ICAM-1. ICAM-1 is a membrane-bound glycoprotein that plays an essential role during immune response, such as leukocyte trafficking.<sup>80</sup> ICAM-1 is expressed in endothelial cells, leukocytes, platelets, epithelial cells, and glial cells. It functions in cell adhesion, migration, and aggregation; and its activity and

expression are usually low when inflammation is absent.<sup>81</sup>

In diabetes, leukocyte adhesion to the retinal endothelium is the primary mechanism of leukostasis, presumably mediated by the up-regulation of ICAM-1. NF- $\kappa$ B activation increased *ICAM-1* expression. A high level of ICAM-1-induced leukocyte adhesion to retinal vascular endothelium via E- and P-selectin causes leukostasis in the retinal vasculature.<sup>82,83</sup> Hence, increased leukostasis is associated with enhanced vascular permeability.<sup>84–87</sup> Furthermore, the

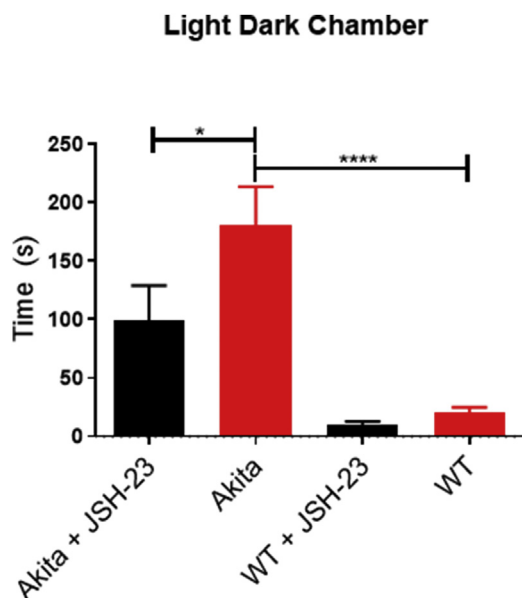


**Figure 11** The light-dark chamber movement test for Akita and wild-type (WT) mice treated with JSH-23. Assessment of vision-guided behavior as assessed via mice movement from the light chamber to the dark chamber.  $n = 8$ . \* $P < 0.05$ , \*\*\*\* $P < 0.0001$ .

inhibition of ICAM-1 reduces retinal vascular leakage and leukocyte adhesion in the streptozotocin-induced diabetic rat.<sup>88</sup> Prominent inflammatory mediators such as iNOS, COX-2, and ICAM-1, are elevated in diabetic retinæ, as also shown in this study. These molecules have been associated with BRB breakdown, leading to increased retinal vascular permeability that potentially contributes to IOP elevation. High glucose down-regulated the expression of *connexin-43*, and 26, thus reducing the intercellular communication between gap junctions. Decreased cell-cell communication is associated with BRB dysfunction.<sup>89</sup> In addition, low expression of *connexin-43* is concurrently related to down-regulation of other junctional proteins (eg, occludin and zonula occludens protein 1).<sup>89</sup> Importantly, the suppressive effect of diabetes supports a transcriptional effect on the status of the occludin rather than a post-transcriptional one.<sup>90</sup> Various regulatory mechanisms highly influence the *connexin-43* gene and its mRNA expression.<sup>91–95</sup>

Retinal pigment epithelium and retinal endothelial cells constitute a critical component of the BRB. Inflammation can lead to subretinal and intraretinal fluid accumulation. Numerous mechanisms have been implicated in dysfunction of the endothelial cells in diabetes. BRB breakdown is strongly associated with the release of proinflammatory factors, such as iNOS, and elevated levels of inflammatory mediators play a definitive role in raising the IOP. In addition, elevated IOP is linked with up-regulation of hypoxia-inducible factor-1 $\alpha$ , tumor necrosis factor- $\alpha$ , ILs, and vascular endothelial growth factor.<sup>96</sup>

## Conclusions

The incidence of T1D is rising, and glycemic variability is becoming more common among young children. This has long-term implications for the health and well-being of diabetic patients. Research has identified several potential options to cure diabetes but so far none of them has shown any concrete outcome.<sup>97–102</sup> Thus, targeted interventions are needed to reduce the risk of long-term T1D-related complications and improve patient quality of life. NF- $\kappa$ B is a key player in the inflammatory process; thus, strategies inhibiting NF- $\kappa$ B have potential therapeutic applications in fighting against T1D. This study showed that inhibition of NF- $\kappa$ B significantly diminished cell-junctional molecule degradation in the retinæ of Akita mice, thereby decreasing vascular permeability and retinal remodeling (Figure 12). IOP was also mitigated, and visual function improved, as shown by vision-guided behavior test when inflammation in the eye was controlled. It is notable that JSH-23 treatment has been shown to abate the inflammatory response to injury

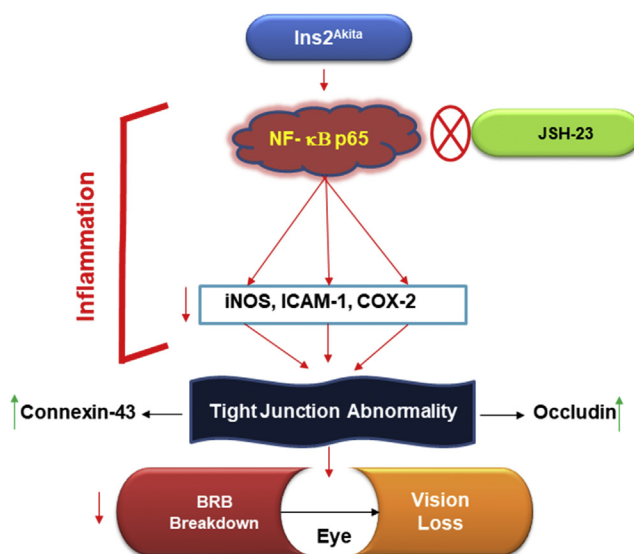


**Figure 12** A schematic showing vision impairment as a result of NF- $\kappa$ B-initiated ocular inflammation during type 1 diabetes. The hyperglycemic environment leads to dysregulation of glucose homeostasis, causing significant increase in inflammatory mediators, such as inducible nitric oxide synthase (iNOS), intercellular adhesion molecule (ICAM)-1, and cyclooxygenase (COX)-2, in the retinæ and concomitant NOD-like receptor family pyrin domain-containing 3 (NLRP3) activation. The resultant inflammatory signature induces degradation of the junctional protein molecules and concurrent death of the retinal cells via pyroptosis. The structural and physiological alterations in the retinal vasculature result in a corresponding decrease in the contents responsible for retinovascular junction integrity, encompassing junctional molecules (connexin-43 and occludin), leading to retinal remodeling. The assembly of NF- $\kappa$ B-initiated NLRP3 inflammasome eventually leads to the derailment of the blood-retinal barrier (BRB), causing vision impairment and blindness. Treatment with JSH-23, an inhibitor of NF- $\kappa$ B p65 subunit, mitigates the debilitating effects of diabetic retinopathy because JSH-23 can decrease inflammatory mediators significantly, thus protecting the retina during diabetes.

in other model systems.<sup>103</sup> It is also worth mentioning that various types of both steroidal and nonsteroidal (nonsteroidal anti-inflammatory drugs) agents have been demonstrated to inhibit NF- $\kappa$ B, but their actions are highly pleiotropic.<sup>104,105</sup> Therefore, one of the major challenges facing scientists is to develop NF- $\kappa$ B inhibitor(s) aimed at treating different diseases based on their ability to target specific pathway(s) in specific disease condition(s) such as DR, with small molecules like JSH-23, thereby avoiding the risk of undesired clinical adverse effects. We hope that the findings of this study will lead the way in validating newer approaches in the near future. This study advances understanding of the role of inflammation in DR. However, additional studies are needed to determine the best way to deliver the JSH-23 compound or its versions directly into the eye in a long-acting manner.

## Acknowledgments

We thank members of The Eye and Vision Science Laboratory, Department of Physiology, University of Louisville School of Medicine, Louisville, KY for continuous support and encouragement. *The father of the senior author passed away in September 2020. This paper is dedicated to his memory.*

## Author Contributions

M.S. and S.C.T. designed the study; R.P.H., H.S.S., and A.K.G. acquired the data; M.S., R.P.H., and H.S.S. analyzed the data; M.S. and R.P.H. prepared the manuscript; M.S., R.P.H., and H.S.S. revised the manuscript; and M.S. supervised the study and finalized the manuscript; all authors read and approved the final version of the manuscript before its submission.

## References

- Pettitt DJ, Talton J, Dabelea D, Divers J, Imperatore G, Lawrence JM, Liese AD, Linder B, Mayer-Davis EJ, Pihoker C, Saydah SH, Standiford DA, Hamman RF: Prevalence of diabetes in U.S. youth in 2009: the SEARCH for diabetes in youth study. *Diabetes Care* 2014, 37:402–408
- Dabelea D, Bell RA, D'Agostino RB Jr, Imperatore G, Johansen JM, Linder B, Liu LL, Loots B, Marcovina S, Mayer-Davis EJ, Pettitt DJ, Waitzfelder B: Incidence of diabetes in youth in the United States. *JAMA* 2007, 297:2716–2724
- Vehik K, Hamman RF, Lezotte D, Norris JM, Klingensmith G, Bloch C, Rewers M, Dabelea D: Increasing incidence of type 1 diabetes in 0- to 17-year-old Colorado youth. *Diabetes Care* 2007, 30: 503–509
- Streisand R, Monaghan M: Young children with type 1 diabetes: challenges, research, and future directions. *Curr Diabet Rep* 2014, 14:520
- Spencer BG, Estevez JJ, Liu E, Craig JE, Finnie JW: Pericytes, inflammation, and diabetic retinopathy. *Inflammopharmacology* 2020, 28:697–709
- Homme RP, Singh M, Majumder A, George AK, Nair K, Sandhu HS, Tyagi N, Lominadze D, Tyagi SC: Remodeling of retinal architecture in diabetic retinopathy: disruption of ocular physiology and visual functions by inflammatory gene products and pyroptosis. *Front Physiol* 2018, 9:1268
- Vaziri K, Schwartz SG, Relhan N, Kishor KS, Flynn HW Jr: New therapeutic approaches in diabetic retinopathy. *Rev Diabet Stud* 2015, 12:196–210
- Safi SZ, Qvist R, Kumar S, Batumalaie K, Ismail IS: Molecular mechanisms of diabetic retinopathy, general preventive strategies, and novel therapeutic targets. *Biomed Res Int* 2014, 2014:801269
- Miyahara S, Kiryu J, Miyamoto K, Hirose F, Tamura H, Yoshimura N: Alteration of leukocyte-endothelial cell interaction during aging in retinal microcirculation of hypertensive rats. *Jpn J Ophthalmol* 2006, 50:509–514
- Liu T, Zhang L, Joo D, Sun S-C: NF- $\kappa$ B signaling in inflammation. *Signal Transduction Targeted Ther* 2017, 2:17023
- Baltimore D: Discovering NF-kappaB. *Cold Spring Harbor Perspect Biol* 2009, 1:a000026
- Hoffmann A, Natoli G, Ghosh G: Transcriptional regulation via the NF-kappaB signaling module. *Oncogene* 2006, 25:6706–6716
- Kumar A, Negi G, Sharma SS: JSH-23 targets nuclear factor-kappa B and reverses various deficits in experimental diabetic neuropathy: effect on neuroinflammation and antioxidant defence. *Diabetes Obesity Metabol* 2011, 13:750–758
- Shin HM, Kim MH, Kim BH, Jung SH, Kim YS, Park HJ, Hong JT, Min KR, Kim Y: Inhibitory action of novel aromatic diamine compound on lipopolysaccharide-induced nuclear translocation of NF-kappaB without affecting IkappaB degradation. *FEBS Lett* 2004, 571:50–54
- Shirato K, Koda T, Takanari J, Sakurai T, Ogasawara J, Imaizumi K, Ohno H, Kizaki T: Anti-inflammatory effect of ETAS(R)50 by inhibiting nuclear factor-kappaB p65 nuclear import in ultraviolet-B-irradiated normal human dermal fibroblasts: evidence-based complementary and alternative medicine. *eCAM* 2018, 2018:5072986
- Wang Q, Dong X, Li N, Wang Y, Guan X, Lin Y, Kang J, Zhang X, Zhang Y, Li X, Xu T: JSH-23 prevents depressive-like behaviors in mice subjected to chronic mild stress: effects on inflammation and antioxidant defense in the hippocampus. *Pharmacol Biochem Behav* 2018, 169:59–66
- Arias-Salvatierra D, Silbergeld EK, Acosta-Saavedra LC, Calderon-Aranda ES: Role of nitric oxide produced by iNOS through NF- $\kappa$ B pathway in migration of cerebellar granule neurons induced by lipopolysaccharide. *Cell Signal* 2011, 23:425–435
- Cai Y, Li W, Tu H, Chen N, Zhong Z, Yan P, Dong J: Curcuminolide reduces diabetic retinal vascular leukostasis and leakage partly via inhibition of the p38MAPK/NF-kappa B signaling. *Bioorg Med Chem Lett* 2017, 27:1835–1839
- Haurigot V, Villacampa P, Ribera A, Llombart C, Bosch A, Nacher V, Ramos D, Ayuso E, Segovia JC, Bueren JA, Ruberte J, Bosch F: Increased intraocular insulin-like growth factor-I triggers blood-retinal barrier breakdown. *J Biol Chem* 2009, 284: 22961–22969
- Coughlin BA, Feenstra DJ, Mohr S: Müller cells and diabetic retinopathy. *Vis Res* 2017, 139:93–100
- Leal EC, Martins J, Voabil P, Liberal J, Chiavaroli C, Bauer J, Cunha-Vaz J, Ambrósio AF: Calcium dobesilate inhibits the alterations in tight junction proteins and leukocyte adhesion to retinal endothelial cells induced by diabetes. *Diabetes* 2010, 59:2637–2645
- Mugisho OO, Green CR, Zhang J, Binz N, Acosta ML, Rakoczy E, Rupenthal ID: Immunohistochemical characterization of connexin43 expression in a mouse model of diabetic retinopathy and in human donor retinas. *Int J Mol Sci* 2017, 18:2567
- Barber AJ, Antonetti DA, Kern TS, Reiter CE, Soans RS, Krady JK, Levison SW, Gardner TW, Bronson SK: The Ins2Akita mouse as a model of early retinal complications in diabetes. *Invest Ophthalmol Vis Sci* 2005, 46:2210–2218

24. Cho H, Sobrin L: Genetics of diabetic retinopathy. *Curr Diabetes Rep* 2014, 14:515
25. Wang J, Takeuchi T, Tanaka S, Kubo SK, Kayo T, Lu D, Takata K, Koizumi A, Izumi T: A mutation in the insulin 2 gene induces diabetes with severe pancreatic beta-cell dysfunction in the Mody mouse. *J Clinical Invest* 1999, 103:27–37
26. Izumi T, Yokota-Hashimoto H, Zhao S, Wang J, Halban PA, Takeuchi T: Dominant negative pathogenesis by mutant proinsulin in the Akita diabetic mouse. *Diabetes* 2003, 52:409–416
27. Han Z, Guo J, Conley SM, Naash MI: Retinal angiogenesis in the Ins2(Akita) mouse model of diabetic retinopathy. *Invest Ophthalmol Vis Sci* 2013, 54:574–584
28. Robinson R, Barathi VA, Chaurasia SS, Wong TY, Kern TS: Update on animal models of diabetic retinopathy: from molecular approaches to mice and higher mammals. *Dis Model Mech* 2012, 5:444–456
29. Committee for the Update of the Guide for the Care and Use of Laboratory Animals; National Research Council: Guide for the Care and Use of Laboratory Animals: Eighth Edition. Washington, DC, National Academies Press, 2011
30. Rasband WS: Image J. National Institutes of Health 1997–2008.
31. Mishra PK, Tyagi N, Sen U, Joshua IG, Tyagi SC: Synergism in hyperhomocysteinemia and diabetes: role of PPAR gamma and tempol. *Cardiovasc Diabetol* 2010, 9:49
32. Ozkok A, Ravichandran K, Wang Q, Ljubanovic D, Edelstein CL: NF- $\kappa$ B transcriptional inhibition ameliorates cisplatin-induced acute kidney injury (AKI). *Toxicol Lett* 2016, 240:105–113
33. Barbetti F, Colombo C, Haataja L, Cras-Méneur C, Bernardini S, Arvan P: Hyperglucagonemia in an animal model of insulin- deficient diabetes: what therapy can improve it? *Clin Diabetes Endocrinol* 2016, 2:11
34. Zhang P: Glucose tolerance test in mice. *Bio-Protocol* 2011, 1:e159
35. Shigemoto-Kuroda T, Oh JY, Kim DK, Jeong HJ, Park SY, Lee HJ, Park JW, Kim TW, An SY, Prockop DJ, Lee RH: MSC-derived extracellular vesicles attenuate immune responses in two autoimmune murine models: type 1 diabetes and uveoretinitis. *Stem Cell Rep* 2017, 8:1214–1225
36. Zietzer A, Niepmann ST, Camara B, Lenart MA, Jansen F, Becher MU, Andrié R, Nickenig G, Tiyerili V: Sodium thiocyanate treatment attenuates atherosclerotic plaque formation and improves endothelial regeneration in mice. *PLoS One* 2019, 14: e0214476-e
37. Asokan P, Mitra RN, Periasamy R, Han Z, Borrás T: A naturally fluorescent Mgp transgenic mouse for angiogenesis and glaucoma longitudinal studies. *Invest Ophthalmol Visual Sci* 2018, 59:746–756
38. Schneider CA, Rasband WS, Eliceiri KW: NIH Image to ImageJ: 25 years of image analysis. *Nat Methods* 2012, 9:671–675
39. Ehlers JP, Wang K, Vasanji A, Hu M, Srivastava SK: Automated quantitative characterisation of retinal vascular leakage and microaneurysms in ultra-widefield fluorescein angiography. *Br J Ophthalmol* 2017, 101:696–699
40. Heldermon CD, Hennig AK, Ohlemiller KK, Ogilvie JM, Herzog ED, Breidenbach A, Vogler C, Wozniak DF, Sands MS: Development of sensory, motor and behavioral deficits in the murine model of Sanfilippo syndrome type B. *PLoS One* 2007, 2:e772
41. Hennig AK, Ogilvie JM, Ohlemiller KK, Timmers AM, Hauswirth WW, Sands MS: AAV-mediated intravitreal gene therapy reduces lysosomal storage in the retinal pigmented epithelium and improves retinal function in adult MPS VII mice. *Mol Ther* 2004, 10: 106–116
42. Collin GB, Gogna N, Chang B, Damkham N, Pinkney J, Hyde LF, Stone L, Naggert JK, Nishina PM, Krebs MP: Mouse models of inherited retinal degeneration with photoreceptor cell loss. *Cells* 2020, 9:931
43. Kamat PK, Kalani A, Givvimani S, Sathnur PB, Tyagi SC, Tyagi N: Hydrogen sulfide attenuates neurodegeneration and neurovascular dysfunction induced by intracerebral-administered homocysteine in mice. *Neuroscience* 2013, 252:302–319
44. Sun J, Huang P, Liang J, Li J, Shen M, She X, Feng Y, Luo X, Liu T, Sun X: Cooperation of Rel family members in regulating A $\beta$ 1-40-mediated pro-inflammatory cytokine secretion by retinal pigment epithelial cells. *Cell Death Dis* 2017, 8:e3115
45. Kanczkowski W, Chatzigeorgiou A, Grossklaus S, Sprott D, Bornstein SR, Chavakis T: Role of the endothelial-derived endogenous anti-inflammatory factor Del-1 in inflammation-mediated adrenal gland dysfunction. *Endocrinology* 2013, 154: 1181–1189
46. Cummings KL, Tarleton RL: Inducible nitric oxide synthase is not essential for control of Trypanosoma cruzi infection in mice. *Infect Immun* 2004, 72:4081–4089
47. He T, Xing Y-Q, Zhao X-H, Ai M: Interaction between iNOS and COX-2 in hypoxia-induced retinal neovascularization in mice. *Arch Med Res* 2007, 38:807–815
48. Chaurasia SS, Lim RR, Parikh BH, Wey YS, Tun BB, Wong TY, Luu CD, Agrawal R, Ghosh A, Mortellaro A, Rackoczy E, Mohan RR, Barathi VA: The NLRP3 inflammasome may contribute to pathologic neovascularization in the advanced stages of diabetic retinopathy. *Sci Rep* 2018, 8:2847
49. Kihara AH, Mantovani de Castro L, Moriscot AS, Hamassaki DE: Prolonged dark adaptation changes connexin expression in the mouse retina. *J Neurosci Res* 2006, 83:1331–1341
50. Luo Y, Xiao W, Zhu X, Mao Y, Liu X, Chen X, Huang J, Tang S, Rizzolo LJ: Differential expression of claudins in retinas during normal development and the angiogenesis of oxygen-induced retinopathy. *Invest Ophthalmol Vis Sci* 2011, 52: 7556–7564
51. George AK, Behera J, Kelly KE, Mondal NK, Richardson KP, Tyagi N: Exercise mitigates alcohol induced endoplasmic reticulum stress mediated cognitive impairment through ATF6-Herp signaling. *Sci Rep* 2018, 8:5158
52. George AK, Homme RP, Majumder A, Tyagi SC, Singh M: Effect of MMP-9 gene knockout on retinal vascular form and function. *Physiol Genomics* 2019, 51:613–622
53. Jun JY, Ma Z, Segar L: Spontaneously diabetic Ins2(+)/Akita: apoE-deficient mice exhibit exaggerated hypercholesterolemia and atherosclerosis. *Am J Physiol Endocrinol Metab* 2011, 301: E145–E154
54. Vrankova S, Barta A, Klimentova J, Dvornikova I, Liskova S, Dobesova Z, Pechanova O, Kunes J, Zicha J: The regulatory role of nuclear factor kappa B in the heart of hereditary hypertriglyceridemic rat. *Oxid Med Cell Longev* 2016, 2016:9814038
55. Tien T, Barrette KF, Chronopoulos A, Roy S: Effects of high glucose-induced Cx43 downregulation on occludin and ZO-1 expression and tight junction barrier function in retinal endothelial cells. *Invest Ophthalmol Vi Sci* 2013, 54:6518–6525
56. Hietala K, Harjutsalo V, Forsblom C, Summanen P, Groop PH: Age at onset and the risk of proliferative retinopathy in type 1 diabetes. *Diabetes Care* 2010, 33:1315–1319
57. Yuan Q, Tang W, Zhang X, Hinson JA, Liu C, Osei K, Wang J: Proinsulin atypical maturation and disposal induces extensive defects in mouse Ins2+/Akita beta-cells. *PLoS One* 2012, 7: e35098
58. Chandel NS, Trzyna WC, McClintock DS, Schumacker PT: Role of oxidants in NF-kappa B activation and TNF-alpha gene transcription induced by hypoxia and endotoxin. *J Immunol* 2000, 165: 1013–1021
59. Fitzgerald DC, Meade KG, McEvoy AN, Lillis L, Murphy EP, MacHugh DE, Baird AW: Tumour necrosis factor-alpha (TNF-alpha) increases nuclear factor kappaB (NFkappaB) activity in and interleukin-8 (IL-8) release from bovine mammary epithelial cells. *Vet Immunol Immunopathol* 2007, 116:59–68
60. Renard P, Zachary MD, Bougelet C, Mirault ME, Haegeman G, Remacle J, Raes M: Effects of antioxidant enzyme modulations on interleukin-1-induced nuclear factor kappa B activation. *Biochem Pharmacol* 1997, 53:149–160



61. Qin H, Wilson CA, Lee SJ, Zhao X, Benveniste EN: LPS induces CD40 gene expression through the activation of NF- $\kappa$ B and STAT-1 $\alpha$  in macrophages and microglia. *Blood* 2005, 106: 3114–3122
62. Basu S, Rosenzweig KR, Youmell M, Price BD: The DNA-dependent protein kinase participates in the activation of NF- $\kappa$ B following DNA damage. *Biochem Biophys Res Commun* 1998, 247:79–83
63. Vlahopoulos S, Boldogh I, Casola A, Brasier AR: Nuclear factor- $\kappa$ B-dependent induction of interleukin-8 gene expression by tumor necrosis factor  $\alpha$ : evidence for an antioxidant sensitive activating pathway distinct from nuclear translocation. *Blood* 1999, 94:1878–1889
64. Christian F, Smith EL, Carmody RJ: The regulation of NF- $\kappa$ B subunits by phosphorylation. *Cells* 2016, 5:12
65. Gao N, Hibi Y, Cueno M, Asamitsu K, Okamoto T: A-kinase-interacting protein 1 (AKIP1) acts as a molecular determinant of PKA in NF- $\kappa$ B signaling. *J Biol Chem* 2010, 285: 28097–28104
66. Chi W, Chen H, Li F, Zhu Y, Yin W, Zhuo Y: HMGB1 promotes the activation of NLRP3 and caspase-8 inflammasomes via NF- $\kappa$ B pathway in acute glaucoma. *J Neuroinflammation* 2015, 12:137
67. Mattioli I, Sebald A, Bucher C, Charles RP, Nakano H, Doi T, Kracht M, Schmitz ML: Transient and selective NF- $\kappa$ B p65 serine 536 phosphorylation induced by T cell costimulation is mediated by I- $\kappa$ B kinase  $\beta$  and controls the kinetics of p65 nuclear import. *J Immunol* 2004, 172:6336–6344
68. Shoelson SE, Lee J, Goldfine AB: Inflammation and insulin resistance. *J Clin Invest* 2006, 116:1793–1801
69. Matsuoka M, Ogata N, Matsuyama K, Yoshikawa T, Takahashi K: Intraocular pressure in Japanese diabetic patients. *Clin Ophthalmol* 2012, 6:1005–1009
70. Xu L, Wang YX, Jonas JB, Wang YS, Wang S: Ocular hypertension and diabetes mellitus in the Beijing Eye Study. *J Glaucoma* 2009, 18: 21–25
71. Albensi BC, Mattson MP: Evidence for the involvement of TNF and NF- $\kappa$ B in hippocampal synaptic plasticity. *Synapse (New York, NY)* 2000, 35:151–159
72. Meffert MK, Chang JM, Wiltgen BJ, Fanselow MS, Baltimore D: NF- $\kappa$ B functions in synaptic signaling and behavior. *Nat Neurosci* 2003, 6:1072–1078
73. Fabio LMR, Frans PN, Gert F: Nitric oxide synthase (NOS) as therapeutic target for asthma and chronic obstructive pulmonary disease. *Curr Drug Target* 2006, 7:721–735
74. Korhonen R, Lahti A, Kankaanranta H, Moilanen E: Nitric oxide production and signaling in inflammation. *Curr Drug Target Inflamm Allergy* 2005, 4:471–479
75. Wang Y, Meng X, Yan H: Niaspan inhibits diabetic retinopathy induced vascular inflammation by downregulating the tumor necrosis factor- $\alpha$  pathway. *Mol Med Rep* 2017, 15:1263–1271
76. Shanmugam N, Gaw Gonzalo IT, Natarajan R: Molecular mechanisms of high glucose-induced cyclooxygenase-2 expression in monocytes. *Diabetes* 2004, 53:795–802
77. Amano H, Ito Y, Suzuki T, Kato S, Matsui Y, Ogawa F, Murata T, Sugimoto Y, Senior R, Kitasato H, Hayashi I, Satoh Y, Narumiya S, Majima M: Roles of a prostaglandin E-type receptor, EP3, in up-regulation of matrix metalloproteinase-9 and vascular endothelial growth factor during enhancement of tumor metastasis. *Cancer Sci* 2009, 100:2318–2324
78. Carmo A, Cunha-Vaz JG, Carvalho AP, Lopes MC: Effect of cyclosporin-A on the blood-retinal barrier permeability in streptozotocin-induced diabetes. *Mediators Inflammation* 2000, 9: 243–248
79. Madonna R, Giovannelli G, Confalone P, Renna FV, Geng YJ, De Caterina R: High glucose-induced hyperosmolarity contributes to COX-2 expression and angiogenesis: implications for diabetic retinopathy. *Cardiovasc Diabetol* 2016, 15:18
80. Carman CV, Sage PT, Sciuto TE, de la Fuente MA, Geha RS, Ochs HD, Dvorak HF, Dvorak AM, Springer TA: Transcellular diapedesis is initiated by invasive podosomes. *Immunity* 2007, 26: 784–797
81. Carnemolla R, Shuvaev VV, Muzykantor VR: Targeting antioxidant and antithrombotic biotherapeutics to endothelium. *Semin Thrombosis Hemostasis* 2010, 36:332–342
82. McLeod DS, Lefer DJ, Merges C, Luty GA: Enhanced expression of intracellular adhesion molecule-1 and P-selectin in the diabetic human retina and choroid. *Am J Pathol* 1995, 147: 642–653
83. Altmann C, Schmidt MHH: The role of microglia in diabetic retinopathy: inflammation, microvasculature defects and neurodegeneration. *Int J Mol Sci* 2018, 19:110
84. Funatsu H, Noma H, Mimura T, Eguchi S, Hori S: Association of vitreous inflammatory factors with diabetic macular edema. *Ophthalmology* 2009, 116:73–79
85. Joussen AM, Poulaki V, Le ML, Koizumi K, Esser C, Janicki H, Schraermeyer U, Kociok N, Fauser S, Kirchhof B, Kern TS, Adamis AP: A central role for inflammation in the pathogenesis of diabetic retinopathy. *FASEB J* 2004, 18:1450–1452
86. Du M, Martin A, Hays F, Johnson J, Farjo RA, Farjo KM: Serum retinol-binding protein-induced endothelial inflammation is mediated through the activation of toll-like receptor 4. *Mol Vis* 2017, 23: 185–197
87. Laha A, Majumder A, Singh M, Tyagi SC: Connecting homocysteine and obesity through pyroptosis, gut microbiome, epigenetics, peroxisome proliferator-activated receptor  $\gamma$ , and zinc finger protein 407. *Can J Physiol Pharmacol* 2018, 96: 971–976
88. Mei XY, Zhou LY, Zhang TY, Lu B, Ji LL: Scutellaria barbata attenuates diabetic retinopathy by preventing retinal inflammation and the decreased expression of tight junction protein. *Int J Ophthalmol* 2017, 10:870–877
89. Roy S, Kim D, Lim R: Cell-cell communication in diabetic retinopathy. *Vis Res* 2017, 139:115–122
90. Antonetti DA, Barber AJ, Khin S, Lieth E, Tarbell JM, Gardner TW; Penn State Retina Research Group: Vascular permeability in experimental diabetes is associated with reduced endothelial occludin content: vascular endothelial growth factor decreases occludin in retinal endothelial cells. *Diabetes* 1998, 47: 1953–1959
91. Li AF, Roy S: High glucose-induced downregulation of connexin 43 expression promotes apoptosis in microvascular endothelial cells. *Invest Ophthalmol Vis Sci* 2009, 50:1400–1407
92. Itahana K, Morikazu Y, Takeya T: Differential expression of four connexin genes, Cx-26, Cx-30.3, Cx-32, and Cx-43, in the porcine ovarian follicle. *Endocrinology* 1996, 137:5036–5044
93. Salameh A: Life cycle of connexins: regulation of connexin synthesis and degradation. *Adv Cardiol* 2006, 42:57–70
94. Salat-Canela C, Sesé M, Peula C, Ramón y, Cajal S, Aasen T: Internal translation of the connexin 43 transcript. *Cell Commun Signal* 2014, 12:31
95. Yuan X, Guo Y, Chen D, Luo Y, Chen D, Miao J, Chen Y: Long non-coding RNA MALAT1 functions as miR-1 sponge to regulate connexin 43-mediated ossification of the posterior longitudinal ligament. *Bone* 2019, 127:305–314
96. Vohra R, Tsai JC, Kolko M: The role of inflammation in the pathogenesis of glaucoma. *Surv Ophthalmol* 2013, 58: 311–320
97. Papu John AS, Kundu S, Pushpakumar S, Amin M, Tyagi SC, Sen U: Hydrogen sulfide inhibits Ca(2+)-induced mitochondrial permeability transition pore opening in type-1 diabetes. *Am J Physiol Endocrinol Metab* 2019, 317:E269–E283
98. Prathipati P, Metreveli N, Nandi SS, Tyagi SC, Mishra PK: Ablation of matrix metalloproteinase-9 prevents cardiomyocytes contractile dysfunction in diabetics. *Front Physiol* 2016, 7:93

99. Veeranki S, Givvimani S, Kundu S, Metreveli N, Pushpakumar S, Tyagi SC: Moderate intensity exercise prevents diabetic cardiomyopathy associated contractile dysfunction through restoration of mitochondrial function and connexin 43 levels in db/db mice. *J Mol Cell Cardiol* 2016, 92:163–173
100. Chaturvedi P, Kalani A, Medina I, Familtseva A, Tyagi SC: Cardiosome mediated regulation of MMP9 in diabetic heart: role of mir29b and mir455 in exercise. *J Cell Mol Med* 2015, 19: 2153–2161
101. Givvimani S, Sen U, Tyagi N, Munjal C, Tyagi SC: X-ray imaging of differential vascular density in MMP-9<sup>-/-</sup>, PAR-1<sup>+/+</sup>, hyperhomocysteinemic (CBS<sup>-/+</sup>) and diabetic (Ins2<sup>-/+</sup>) mice. *Arch Physiol Biochem* 2011, 117:1–7
102. Joshua IG, Zhang Q, Falcone JC, Bratcher AP, Rodriguez WE, Tyagi SC: Mechanisms of endothelial dysfunction with development of type 1 diabetes mellitus: role of insulin and C-peptide. *J Cell Biochem* 2005, 96:1149–1156
103. He Q, Zhang C, Wang L, Zhang P, Ma D, Lv J, Liu F: Inflammatory signaling regulates hematopoietic stem and progenitor cell emergence in vertebrates. *Blood* 2015, 125:1098–1106
104. Gupta SC, Sundaram C, Reuter S, Aggarwal BB: Inhibiting NF-κB activation by small molecules as a therapeutic strategy. *Biochim Biophys Acta* 2010, 1799:775–787
105. Malukiewicz G, Stafiej J, Lesiewska H, Sikorski B: Use of nonsteroidal anti-inflammatory drugs in diabetic retinopathy. *Klinika Oczna* 2016, 118:44–47